

A SIMPLIFIED APPROACH FOR THE DIRECT DETECTION
OF PROTEIN OXIDATION IN MUSCLE USING IN-GEL AND
MICROPLATE ASSAYS

ALI NEJATBAKHSR

A THESIS SUBMITTED TO
THE FACULTY OF GRADUATE STUDIES
IN PARTIAL FULFILLMENT OF THE REQUIRMENTS
FOR THE DEGREE OF
MASTER OF SCIENCE

GRADUATE PROGRAM IN KINESIOLOGY AND HEALTH SCIENCE
YORK UNIVERSITY
TORONTO, ONTARIO

May 2016

© ALI NEJATBAKHSR, 2016

Abstract

Reactive oxygen species (ROS) are emerging as regulators of protein redox states which influence many physiological processes. Current methods for the detection of protein redox states, including mass spectrometry, are expensive and not easily accessible or poorly validated. IRdye800CW Maleimide, a highly sensitive maleimide-based infrared dye, has been reported to detect the redox state of immunoprecipitated proteins in cardiac muscle using modified western blot procedures, but has yet to be validated as a novel tool to detect redox conditions throughout the proteome using common and cost-effective assays. In this study we tested the efficacy of IRDye800CW Maleimide in detecting protein redox state in cardiac muscle using mini-gel SDS-PAGE and an in-well approach. Chemical and heat-induced modifications to cardiac tissue redox states were accurately detected with the dye in cardiac lysates. These findings were also validated against HPLC measures of GSSG content.

Acknowledgements

I would like to start by thanking my supervisor Doctor Christopher Perry for all the support and guidance he has provided me throughout my master's degree. Your mentorship and encouragement has allowed me to reach new heights in my academic career and I am truly thankful for the opportunities you have provided me. Your sense of humour has added to the great experience I have had over the years and while others may have released an angry sigh after hearing one of your jokes for the 20th time, I always managed to crack a smile...mostly at the angry sigh.

To my lab mates Meg, Pat and Sofhia, I would like to thank you three for creating the best lab environment anyone could ask for. All the country music, funny conversations and "insults" have made us way too comfortable around each other. If this was witnessed by other labs they would probably think it's weird. Nevertheless, I am grateful for all the help, support and entertainment you have all given me because it makes all the difference in the world, especially when assays never seem to work.

Thank you all.

Contents

Abstract	ii
Acknowledgements	iii
List of Abbreviations.....	vi
List of Tables.....	viii
List of Figures	ix
Chapter 1: Introduction	1
Chapter 2: Background.....	4
2.A - Redox signaling as a regulator of cellular function.....	4
2A.1 - Sources of Oxidants	4
2A.2 – Redox Signaling	6
2A.3 - Major Redox Buffering Mechanisms	12
2A.4 - Cellular Redox State: Relationship to Cellular Functions.....	13
2B - Current Methods for Determining Protein Redox State	15
2B.1 - Mass Spectrometry	15
2B.2 - GSH:GSSG Ratio	16
2B.3 - Thiol Assay Kits	17
2B.4 - Oxidation-Specific Probes.....	17
2B.5 - Thiol Redox State Detection with DIGE.....	18
2C - Barriers to simplified detection of cellular redox state in tissue lysate	19
Chapter 3: Purpose	21
Chapter 4: Methods	22
Chapter 5: Results	27
Chapter 6: Discussion.....	46
6A - Desalting leads to increased fluorescent signal with IRDye800CW Maleimide	46
6B - Oxidizing and reducing agents may interfere with IRDye800CW Maleimide	47
6C - Effects of Reducing and Oxidizing samples on IRDye800CW Maleimide fluorescence	47
6D - TCEP returns fluorescence of Oxidized samples to Control Levels	48
6E - 49 ⁰ C heat treatment lowers IRDye800CW Maleimide fluorescence	50
6F - 40 ⁰ C heat treatment has no significant effect on IRDye800CW Maleimide fluorescence.....	52
6G - 49 ⁰ C heat significantly increases protein carbonylation while 40 ⁰ C does not.....	53
7A - Conclusions.....	54

7B – Future Directions	55
References	57
Appendix A – Optimization Process for IRDye800CW Maleimide	66
A1. Assay Buffer	66
A2. Incubation Conditions	66
A3. DTT and H ₂ O ₂	67
Appendix B: Supplemental figures	69
Appendix C: Buffers	70
Appendix D: Homogenization protocol	71
Appendix E: Final protocol for treatment with TCEP and H ₂ O ₂	72
Appendix F: BCA protein assay.....	72
Appendix G: Western blotting protocol	74

List of Abbreviations

BCA	Bicinchoninic Acid
BODIPY	boron-dipyrromethene
Cy5	Cyanine5
D	Desalted
ddH ₂ O	double distilled water
DIGE	Difference in Gel Electrophoresis
DNA	Deoxyribonucleic acid
DNPH	2,4-dinitrophenylhydrazine
DTNB	5,5-dithio-bis-(2-nitrobenzoic acid)
DTT	Dithiothreitol
ETC	Electron Transport Chain
FADH ₂	Flavin Adenine Dinucleotide Hydroquinone
GAPDH	Glyceraldehyde 3-phosphate dehydrogenase
Gpx	Glutathione Peroxidase
GR	Glutathione Reductase
Grx	Glutaredoxin
GSH	Reduced Glutathione
GSSG	Oxidized Glutathione
H ₂ O ₂	Hydrogen Peroxide
HPLC	High Performance Liquid Chromatography
kDa	Kilodaltons
MS	Mass Spectrometry
NADPH	Nicotinamide Adenine Dinucleotide Phosphate
NaI	Sodium Iodide
ND	No desalting
NEM	N-ethylmaleimide
NIRF	Near infrared Frequency
nM	nanomolar
nm	nanometer
NO•	Nitric Oxide Radical
NO ₂ •	Nitrogen Dioxide Radical
NO ₃ •	Nitrate Radical
NO	Nitric Oxide
NOS	Nitric Oxide Synthase
NOX	NADPH Oxidase
O ₂ ⁻ •	Superoxide Anion
OH•	Hydroxyl Radical
ONOOH	Peroxynitrite
OPA	o-Pthaldialdehyde
OX	Oxidized
Prx	Peroxiredoxin
PVDF	polyvinyliden fluoride
RED	Reduced

RNS	Reactive Nitrogen Species
ROS	Reactive Oxygen Species
SDS-PAGE	Sodium dodecyl sulfate polyacrylamide gel electrophoresis
-SH	Sulfhydryl
SOD	Superoxide Dismutase
TCEP	tris(2-carboxyethyl)phosphine
Trx	Thioredoxin
XO	Xanthine Oxidase

List of Tables

Table 1. List of Redox-sensitive Proteins Identified in Various Studies

7

List of Figures

Figure 1. Reduced and oxidized forms of thiols	2
Figure 2. Common cellular sources of ROS and RNS	6
Figure 3. Major enzymatic antioxidant system within cells	13
Figure 4. Effects of desalting homogenates prior to dye treatment	29
Figure 5. Effects of desalting on GSH content	30
Figure 6. Quenching effects of reagents on IRDye800CW Maleimide	31
Figure 7. Effects of reducing and oxidizing samples on IRDye800CW in-gel	32
Figure 8. Rescue effects of TCEP on pre-oxidized samples in-gel	34
Figure 9. Rescue effects of TCEP on pre-oxidized samples in plate	35
Figure 10. Rescue effects of TCEP on GSH and GSSG content	36
Figure 11. Effects of 49°C heat treatment on IRDye800CW Maleimide fluorescence using in-gel approach	38
Figure 12. Effects of 49°C heat treatment on IRDye800CW Maleimide fluorescence using in-well approach	39
Figure 13. Effects of 49°C heat treatment on GSH, GSSG and GSH/GSSG ratio	40
Figure 14. Effects of 40°C heat treatment on IRDye800CW Maleimide fluorescence using in-gel approach	42
Figure 15. Effects of 40°C heat treatment on IRDye800CW Maleimide fluorescence using in-well approach	43
Figure 16. Effects of 40°C heat treatment on GSH, GSSG and GSH/GSSG ratio	44
Figure 17. Effects of 40°C and 49°C treatment on protein carbonylation	46

Chapter 1: Introduction

As Earth's atmosphere became increasingly oxidizing over millions of years, organisms acquired specific biological systems to help deal with this change. This highly conserved reduction-oxidation (redox) system has evolved in order to help maintain homeostasis within living organisms to protect against the potentially toxic oxidizing atmosphere through many redox sensitive components in mammals and plants (See table 1). Indeed, it has been established that over-exposure to oxidants beyond the protective limits of the cells can lead to protein dysfunction and cell death¹⁻⁵. Over the last 20 years, however, research has extended the role of redox systems and oxidants to include regulation of many physiological processes. This form of regulation is termed 'redox signaling' and has been implicated in the regulation of many cellular processes including metabolism, transcription, inflammation and cell proliferation^{6,7}.

The ability of redox-sensitive molecules to alternate between the reduced and oxidized state is what prompts much of the signaling processes to occur. A molecule is said to be in the reduced state when it has gained one or more electrons while an oxidized molecule is one that has lost one or more electrons. The key compound in redox biology that is capable of undergoing these reversible electron transfers is the thiol which contains a sulfhydryl (-SH) group². Redox signaling occurs through the interaction of both reactive oxygen species (ROS) and reactive nitrogen species (RNS) with thiols. When exposed to these species thiols undergo a variety of structural changes that lead to altered states and conformations which can ultimately trigger a series of signaling processes within the cell. In addition to reversible forms of oxidation, ROS and RNS are also capable of irreversibly oxidizing a thiol in a permanently oxidized state thereby eliminating the redox signaling capability of the thiol^{2,8}. This typically occurs when higher order

oxidation takes place. Figure 1 shows some of the various oxidized products that form when a thiol is exposed to ROS and RNS.

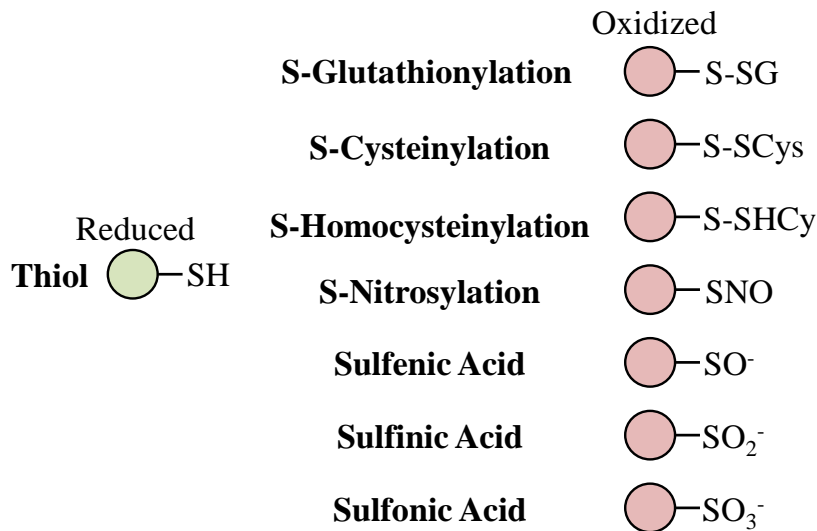


Figure 1 (Adapted from Go et al. 2013)⁸. Reduced and Oxidized forms of Thiols.

When a thiol is exposed to reactive oxygen and nitrogen species, a variety of products can form as shown. Most of the oxidative modifications shown are reversible while sulfenic and sulfonic acids are irreversible forms of oxidation produced in highly oxidizing environments.

ROS and RNS come in many forms which can be categorized as either radical or non-radical species. Radical species, such as the hydroxyl radical (OH•), superoxide anion (O₂⁻•), nitric oxide (NO•) and nitrogen oxides (NO₂•/NO₃•), contain an unpaired electron and are highly unstable. As such, they are typically more reactive and have shorter life spans since they strip away electrons from surrounding sources, such as proteins, lipids and nucleic acids, in order to gain stability⁹. In doing so, these components undergo oxidation and are capable of causing further oxidation until two radical species join to terminate the cycle. Non-radical species include hydrogen peroxide (H₂O₂) and peroxynitrite (ONOOH) and do not contain any unpaired electrons yet still show high

reactivity towards thiols. While non-radical species are generally less reactive than radical species, they have a longer life span and are capable of diffusing membranes which may lead to oxidative modifications and signaling processes beyond their initial site of production⁹. Of the few chemical compounds that contain thiols, cysteine residues have been the most extensively studied in terms of redox biology. This amino acid contains a thiol group that is highly susceptible to reactions by ROS/RNS^{10,2}. Exposure of thiols to these reactive species can alter the thiol to a number of possible oxidized by-products shown above thereby leading to a change in protein structure and function. Indeed, many cellular processes are sensitive to redox signaling including the regulation of transcription factors, inflammatory responses, metabolism, and cell proliferation and differentiation^{2,7,11}. Thus, determining the full mechanisms behind these and other processes necessitates an understanding of the role played by redox signaling and doing so requires sensitive methodologies to measure and detect thiol redox states in both cell culture and animal models.

Chapter 2: Background

2.A - Redox signaling as a regulator of cellular function

2A.1 - Sources of Oxidants

ROS and RNS are highly reactive radical or non-radical molecules produced within organisms as a byproduct of many physiological factors and they serve many essential functions. There are a number of in vivo sources of ROS and RNS and the list below highlights some of the major contributors to their production.

The NOX family of nicotinamide adenine dinucleotide phosphate (NADPH) oxidases are a group of enzymes capable of transferring electrons from NADPH to oxygen to produce superoxide in multiple cellular compartments including plasma membrane, nuclei, cytosol and in the mitochondria (Figure 2)^{12,13}. While superoxide is the immediate product of NOX enzymes, H₂O₂ can be formed from the spontaneous or enzymatic dismutation of superoxide¹⁴. The balanced production of ROS by the NOX family is important for the regulation of a number of cellular signaling processes such as gene expression, cell differentiation, defense and posttranslational protein modifications^{7,14}. An overproduction of ROS from this source has been associated with cardiovascular disease and impairments in gene transcription¹².

Xanthine oxidase (XO) is a cytosolic enzyme responsible for the breakdown of purines in humans and is a known source of both hydrogen peroxide and superoxide generation within the cell with the former being the major product¹⁵. While low levels of XO-generated ROS play a role in antimicrobial defense, increased levels have been associated with tissue damage and gout^{16,17}.

Nitric oxide synthase (NOS) plays a regulatory role in vascular homeostasis through the coupling of molecular oxygen with L-arginine to produce nitric oxide (NO)¹⁸. When L-arginine levels drop, the enzymatic activity of NOS becomes 'uncoupled' such that NOS activity shifts

towards superoxide production¹⁸. There are various NOS isoforms that are located in a number of different types of cells and tissues, however they all display similar enzymatic activities with the potential to generate ROS and RNS which can lead to cell damage¹⁸.

The electron transport chain (ETC) of the mitochondria is another major source of ROS within cells. Electron carriers derived from Kreb's cycle (NADPH, FADH₂) that are normally transferred down the ETC during oxidative phosphorylation can prematurely 'slip' off of the ETC and bind to free O₂ to produce superoxide which can be converted to H₂O₂^{19,20}. While this list of in vivo sources of ROS and RNS is not exhaustive, it highlights the widespread production and use of these species within cells (Figure 2) in order to maintain homeostasis through 'redox signaling' and in conditions of oxidative stress.

Apart from the physiological sources, ROS and RNS can also be produced by factors beyond the organism itself. These external sources include radiation, ozone, environmental toxins and behaviours such as smoking⁴. It is thought that these factors can not only be a source of ROS but that they can catalyze the formation of ROS and RNS within tissue leading to health risks²¹.

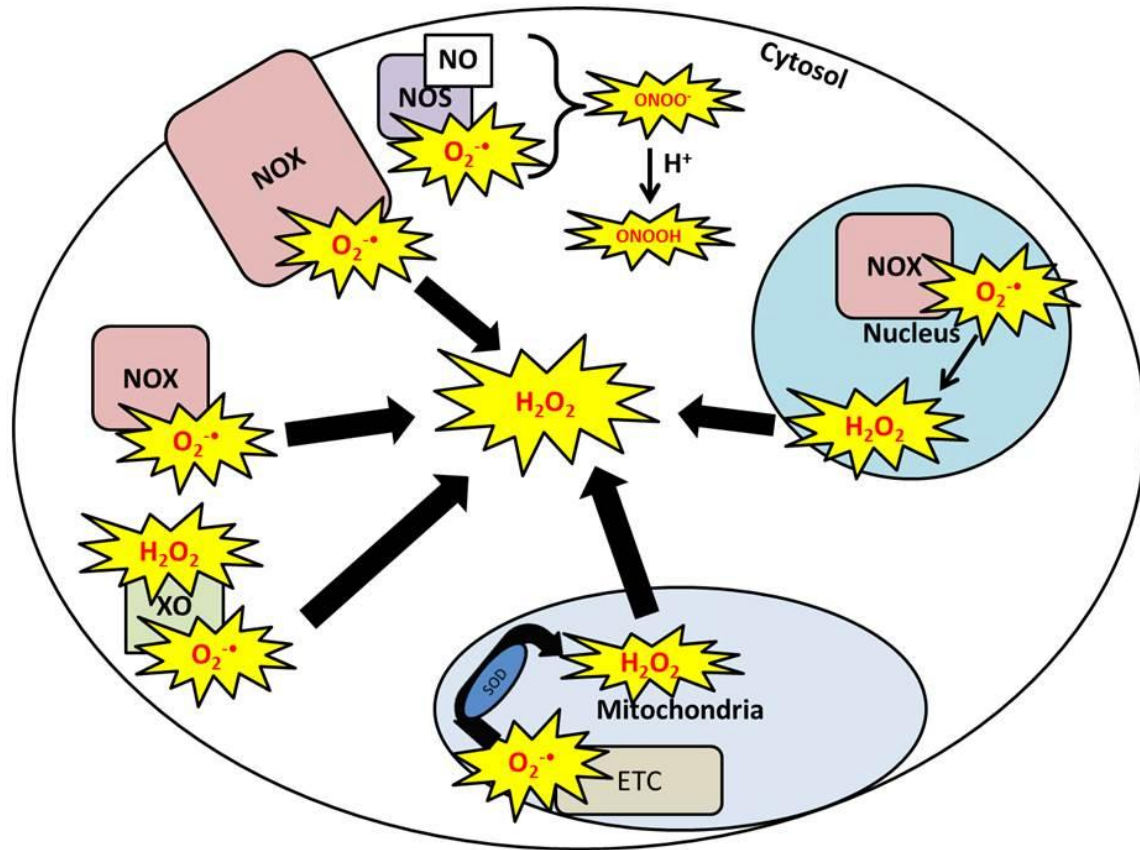


Figure 2. Common Cellular sources of ROS and RNS. NADPH oxidase (NOX) isoforms are located in the nuclei, cytosol and on cell membranes and are capable of producing various forms of ROS and RNS. Nitric oxide (NO) can be combined with superoxide ($O_2^{\bullet-}$) to produce the peroxynitrite anion ($ONOO^-$) which can become protonated to form the non-radical form. Similarly, xanthine oxidase (XO) is a source of both $O_2^{\bullet-}$ and hydrogen peroxide. Electrons slipping from ETC complexes in the mitochondria produce superoxide radicals which can be converted to hydrogen peroxide through the enzyme superoxide dismutase (SOD). Hydrogen peroxide is a more stable form of oxidant and is capable of crossing membranes while superoxide is relatively unstable and localized.

2A.2 – Redox Signaling

ROS and RNS play a dual role in physiological processes and the fate of cells. On one hand there is evidence to suggest a role in signaling responses to maintain homeostasis and the integrity of the cell^{10,22,23}. For example, moderate levels of ROS act as secondary messengers for cell proliferation, cytosolic calcium concentrations, protein phosphorylation and activation of

various transcription factors^{24,25}. On the other hand when ROS and RNS levels go beyond normal, ‘oxidative stress’ can occur leading to impairments in cellular function and apoptosis². These elevated levels of ROS/RNS could then signal adaptations or, if excessive, lead to cellular damage. Thus, alterations in the redox status of cellular components can be thought of as a continuum where small changes could be managed and necessary to maintain normal function while exceeding the healthy threshold can lead to adaptation or impairments.

ROS and RNS have been investigated as mediators of many cellular and physiological processes through reduction and oxidation of protein residues, specifically cysteines¹⁰. The thiol groups on cysteines have an average pKa value of approximately 8.5 which makes them less likely to react with ROS and RNS²⁶. However, this value drops substantially in the presence of other protein domains and in the conditions of the surrounding microenvironment. In this case, cysteine thiols typically have a pKa value of 4 or less depending on the environment and they exist in the thiolate anion form (S⁻) at plasma pH (7.1)¹¹. This renders the cysteine more reactive with ROS and RNS compared to the thiol (SH) form²⁷. The resulting perturbations in the redox state of cysteine thiols can alter the shape, structure and, ultimately, the function of proteins, lipids and nucleic acids²⁰ and can lead to a sequence of physiological events through redox signaling pathways. Table 1 shows some of the redox sensitive proteins that have been investigated.

Table 1. List of Redox-sensitive Proteins Identified in Various Studies²⁸⁻³³.

Function	Protein
DNA repair	Ku80
	MCM6
	80kDa MCM3-associated protein

Metabolism	Acyl-CoA dehydrogenase
	Alcohol dehydrogenase 1 and 2B4
	Aldose 1-epimerase
	Amino acid transporter E16
	C1-tetrahydrofolate synthase
	Carnitine acetyltransferase
	Catechol-O-methyltransferase
	Complex III of mitochondrial electron transport chain
	Enolase 1 and 2
	GAPDH
	Glucosidase alpha
	Iron-sulfur protein assembly 1 homologue
	Malate dehydrogenase
	Mitochondrial creatine kinase
	Neutral amino acid transporter B
	Phosphoglycerate kinase
	PTP1B
	Pyruvate dehydrogenase, E3 binding protein
	Pyruvate dehydrogenase kinase, isoenzyme 2
	Voltage dependent anion channel 1
Antioxidant System	2-Cys peroxiredoxin

	Ascorbate peroxidase
	manganese superoxide dismutase
	thioredoxin-dependent preoxidase 1
Nuclear Transport	Importin 9
	Karyopherin Beta 1
	Ran
	20S proteasome alpha subunits A1, B1, G1 and E
Protein Homeostasis	Calnexin
	Calreticulin
	ER-Golgi intermediate compartment protein1
	Hs7p75 (TRAP1)
	Hsp90-alpha
	Tripeptidyl Peptidase II
	Ubiquitin-activating enzyme E1
Protein Synthesis	Gln-tRNA synthetase
	hnRNP U protein
	Met-tRNA synthetase
	Ribosomal protein S3 and S6
	Thr-tRNA synthetase
	U2 small nuclear RNA auxiliary factor 1
Transcription and Translation	Elongation factor 1-alpha
	Elongation factor 1B alpha-subunit 2

	Translation elongation factor Ts
	Nrf2
	Yap1p
Post-translational Control/Modification	Calreticulin 1
	Chaperonin-60 alpha
	Cytosolic Cyclophilin
	Phosphoprotein phosphatase
	Protein disulfide isomerase-like protein
Cytoskeleton	Actin 7
	Tubulin alpha-6 chain
	Tubulin beta-2
Redox Homeostasis	Glutathione transferase Mu 3
	Peroxiredoxin I
Signaling	Aspartyl β -hydroxylase
	Cardiotrophin-like cytokine factor 1
	IQGAP1
	G protein, β polypeptide 2
	PI-3-kinase, catalytic subunit
	Protein phosphatase PP1, catalytic subunit
	SH2 domain-containing adapter protein F
Vesicle transport	Rab1a
	Rab10
	Rab33b

As previously stated, an important requirement for redox signaling is the ability of a thiol to alternate between reduced and oxidized states. The reversibility of redox status provides a mechanism by which proteins and enzymes can activate or deactivate their activity. For instance, it has been established that protein-tyrosine phosphatases contain active site cysteines that can become oxidized thereby inactivating the enzyme and preventing dephosphorylation of targets³⁴. Similarly, certain metabolic enzymes, including GAPDH, have been shown to be regulated by changes in redox status of their active site cysteines³⁵. In considering that many caspases, kinases, phosphatases and proteases contain active site cysteines², redox signaling may play a potential role in being a significant regulator of many cellular processes via reversible oxidation through changes shown in Figure 1.

Disulfide bonds are known to cause signaling by changing protein structure and protein folding. Cysteines are a critical part of secondary, tertiary and quaternary protein structure due to their ability to form disulfide bonds between other cysteines². Changing the protein or enzyme structure through changes in cysteine thiol redox state can ultimately lead to altered function and provide yet another means for redox signaling to occur.

When considering the large number of redox sensitive proteins and the various signaling cascades that may occur in response to varying levels of oxidation, researchers who are interested in determining the effects of ROS and RNS on cellular function may benefit from methods that allow accurate determination of whole cell redox states which can then be used in concert with protein-specific measures of redox status. Section B will cover some of the common methods used to detect changes in redox state.

2A.3 - Major Redox Buffering Mechanisms

Under normal healthy conditions the rate of ROS/RNS production is balanced by their removal with the help of a number of enzymatic and non-enzymatic antioxidant systems. Examples of enzymatic antioxidants include superoxide dismutase (SOD) which catalyzes the breakdown of the superoxide radical into hydrogen peroxide and catalase which converts hydrogen peroxide into water. While there are a number of non-enzymatic redox buffering mechanisms, such as vitamins C and E, the major one is reduced glutathione (GSH). GSH is the most abundant redox buffer in cells and is present in millimolar concentrations²⁵. If a protein thiol undergoes reversible oxidation, GSH is able to donate its electrons via glutaredoxin (Grx) to oxidized proteins in order to return them to the reduced state³⁶. In doing so, GSH itself becomes oxidized to form a thyl radical (GS•) which can react with other GS• molecules to form oxidized glutathione (GSSG)²⁵. GSSG can then be reduced back to GSH by the glutathione reductase (GR) enzyme which depends on NADPH as the source of electrons²⁵.

Thioredoxin (Trx) also acts as a redox buffering mechanism in both a direct and indirect fashion. Trx can directly reduce oxidized proteins by transferring its electrons and also acts to indirectly convert H₂O₂ to water through peroxiredoxin (Prx)³⁶. For both redox buffering pathways (Grx and Trx), NADPH is the master reducing system derived from the pentose phosphate pathway of glucose metabolism. This reducing agent provides the electrons necessary for the majority of antioxidant defenses within cells³⁶. Figure 3 represents this defense system. When the production of ROS/RNS exceeds the antioxidant capacity of the cell, oxidative/nitrosative stress can occur leading to cell death and disease.

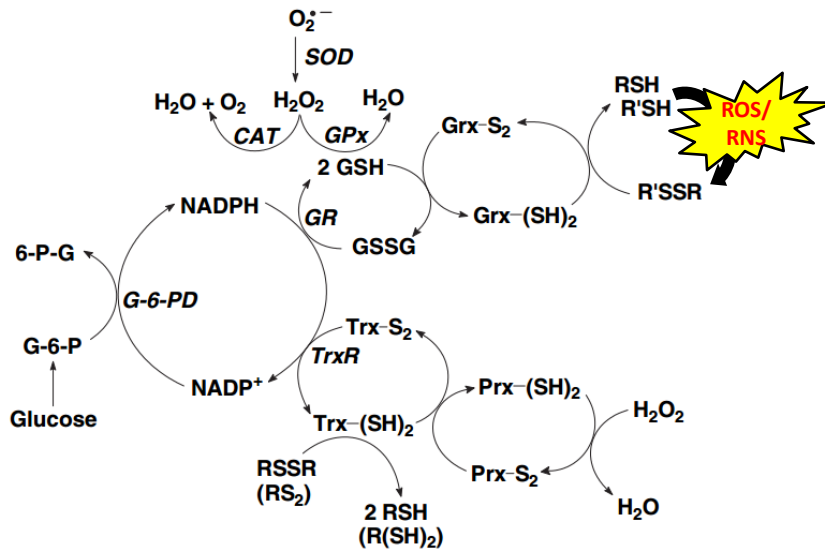


Figure 3. Major Enzymatic Antioxidant System within Cells. NADPH provides the reducing power to most of the antioxidant pathways in cells. Oxidized glutathione (GSSG) accepts an electron from NADPH to become reduced (GSH) with the help of glutathione reductase (GR). GSH can either donate its electron to glutathione peroxidase (Gpx) which converts H_2O_2 to water or it can donate the electron to glutaredoxin (Grx) which then donates the electron to an oxidized protein, thereby reducing it. Thioredoxin (Trx) can also accept electrons from NADPH to directly reduce proteins or by indirectly converting H_2O_2 to water through peroxiredoxin (Prx) (adapted from Ng et al)³⁷.

It is through this antioxidant system that cysteines are regulated as part of redox signaling.

Ultimately, these redox recycling mechanisms dictate the redox state of a given protein and indeed the entire redox proteome which is often referred to as ‘cellular redox state’.

2A.4 - Cellular Redox State: Relationship to Cellular Functions

Physiological signaling processes often involve more than a single regulatory site.

Therefore, when attempting to understand these processes, it becomes useful to consider overall

changes as well. Similarly when considering redox signaling pathways, it is important to investigate global changes in redox states in response to stressors since 1) it may be useful to determine large-scale changes in redox states after a stress has been introduced to a particular site and 2) small changes in redox states can trigger a cascade of signaling events that alter the redox states of multiple sites within the cell.

Instances where a researcher may find it helpful to measure cellular redox states may include normal daily fluxes in redox states in response to mild stressors. For example, in a study by Anderson et al. it was found that rodents on a 3-day high-fat diet had significantly elevated levels of mitochondrial H₂O₂ emission. In addition, they found that the GSH/GSSG ratio, an indirect measure of whole cell oxidation, was significantly lower in high-fat fed mice indicating a more oxidized state³⁸. Therefore, acute challenges can alter whole-cell redox states and measuring this parameter would provide insight to these changes.

Research benefiting from the determination of whole cell redox states can also be extended to pathophysiological conditions. Changes in global redox status of cells have been implicated in a variety of chronic diseases. Oxidative and nitrosative stress caused by overproduction of ROS and RNS has been studied due to their role in aging^{39,40}, muscular dystrophies⁴¹⁻⁴⁴, metabolic disorders⁴⁵⁻⁴⁸, neurodegenerative disorders^{3,49} and cancer^{20,50-52}. A common characteristic shared by these diseases is an increased rate of overall ROS/RNS production with a concomitant decrease in antioxidant defense systems resulting in a cycle of increasing oxidative damage and decreased cell function which ultimately leads to DNA and protein damage on a whole-cell level. For example, several studies have found associations with oxidative stress and neurodegenerative disorders such as Alzheimer's and Parkinson's disease, in which oxidative damage to proteins, lipids and DNA was significantly higher in neuronal cells compared to controls^{3,53-64}. When considering the high reactivity of ROS/RNS with lipids,

proteins and nucleic acids, it should come as no surprise that the accumulation of these factors can cause damage that may lead to altered cell-signaling and impaired function which could ultimately lead to illness. Assessment of oxidative damage in diseases like those mentioned above was based on methods targeting specific markers of oxidative stress (carbonylation for protein oxidation, 4-Hydroxynonenal for lipid oxidation and 8-hydroxy-2'-deoxyguanosine for DNA oxidation) rather than a whole-cell approach to determine overall cellular redox state. To gain a better understanding on the relationship between oxidative states and disease, it may be necessary to consider methods that measure total changes in cellular redox state as opposed to a single marker of oxidation.

2B - Current Methods for Determining Protein Redox State

2B.1 - Mass Spectrometry

Given the critical importance of ROS/RNS in cell signaling and health, several methods have been developed to accurately detect the type and extent of redox modifications on biological samples. Mass spectrometry (MS) is one of the most commonly used techniques in metabolic research and has been growing in popularity over the years^{65,66}. As such, it has been used in a variety of studies as a method to determine redox modifications with high specificity⁶⁷⁻⁶⁹. A typical MS procedure works by first ionizing a sample, forming fragments of charged particles. These particles are then detected based on their mass-to-charge ratio which is then correlated to known masses to determine the chemical composition in the original sample. As an analytical tool, MS offers a number of distinct advantages including high specificity, providing information on molecular weight and isotopic abundance of chemical species, and the ability to be combined with a number of other separation techniques (i.e. chromatography). While this

method is appealing due to its sensitivity and accuracy, typical mass spectrometers can cost upwards of hundreds of thousands of dollars and require a high degree of technical training for its implementations. Hence its use is not accessible for many laboratories and is limited to many researchers due to the high levels of training requirements.

2B.2 - GSH:GSSG Ratio

The ratio of reduced glutathione (GSH) to oxidized glutathione (GSSG) is often used as a marker of total protein oxidation within a sample. When proteins are reversibly oxidized (e.g. disulfide bond formation, other), they can be returned back to the reduced state by GSH, which donates an electron to the oxidized protein to cause reduction³⁶. As mentioned above, GSH transfers its electron to reduce an oxidized protein thiol and becomes converted to GS• which is capable of forming a disulfide bond with a second GS•. This oxidized complex, referred to as GSSG, is incapable of further protein reduction. A low GSH:GSSG is therefore used as a marker for global cellular protein oxidation⁷⁰ and can be determined both colorimetrically, as described below, or by high performance liquid chromatography (HPLC)⁷¹. While a common assumption with this method is that a change in GSH:GSSG ratio will reflect a change in whole-cell redox state, it may be that the assumption does not apply to the entire redox proteome. Direct measures of cellular and protein redox states could reveal surprising heterogeneity across the proteome. Furthermore, the sensitivity of the of 5,5'-dithio-bis-(2-nitrobenzoic acid (DTNB)-linked colorimetric kit for detecting GSSG has been questioned in our own lab and others (data not shown) whilst the more sensitive HPLC is often not accessible to many laboratories.

2B.3 - Thiol Assay Kits

Along with the thiol and oxidation-specific probes mentioned above, various colorimetric and absorbance-based kits are commercially available for researchers interested in measuring thiol content in a sample. These assays typically incorporate a compound that leads to a colour change when reacted with thiols and allows the investigator to determine the thiol concentration through a standard curve. A commonly used assay involves the use DTNB which produces a yellow solution in the presence of thiols thereby allowing researchers to quantify total thiol content in a sample. While simple to use, this method lacks specificity between free thiols and thiol groups on cysteines and would have limited use to investigations that need to discriminate between the two. Many similar colorimetric kits are available that work under the same principle however this method is limited by its sensitivity and specificity when compared to the fluorometric approaches mentioned above. As such, a method that addresses these issues while offering simple, reliable and easy to use protocols would be of benefit to many investigators.

2B.4 - Oxidation-Specific Probes

When proteins become oxidized they can undergo a variety of modifications resulting in a number of different oxidized compounds, such as glutathionylation, carbonylation, nitrosylation or sulfur-based acids, to name a few⁷². Specific probes for each modification are becoming available^{73,74} and are useful for determining the role of a particular modification in redox signaling. For example, Oxyblot kits are commonly used to measure protein carbonylation using western blotting approaches. This assay is based on the reaction of carbonylated proteins with 2,4-dinitrophenylhydrazine (DNPH). While relatively easy to use, these assays have a number of disadvantages. Mainly, they have been criticized for their inability to yield reproducible results which may stem from the degradation of their proprietary components⁷⁵. Furthermore, these

methods do not confirm whole-cell redox state in terms of total thiol oxidation of all forms and limit the researcher by measuring only one form of oxidation.

As an alternative to oxidation product-specific probes, a number of probes specific for reduced thiols with wide spectral ranges and sensitivities have been developed to measure protein redox states. Iodoacetamide and maleimide based probes are commonly used in redox studies as they irreversibly react with reduced thiols at their specified pH ranges. Iodoacetamide dyes, such as boron-dipyrromethene (BODIPY) fluorophores and eosin-5-iodoacetamide, and maleimide dyes such as Cyanine5 (Cy5) and Alexa Fluor 647 C₂ maleimide, have been used for their specificity towards thiol groups and their ability to be incorporated with gel electrophoresis. However, specificity of these dyes towards thiols tends to decline when they are used above a certain concentration⁷⁶ and it has even been reported that iodoacetamide-based dyes react with methionine, tyrosine and histidine which can confound results aimed at measuring reduced thiols⁷⁷. Another disadvantage of these probes is that their emission spectra tend to lie in the visible range. It has been argued that detection in this region, especially near lower wavelengths, leads to low signal-to-noise ratio when compared to images obtained in the near-infrared (NIRF) range⁷⁸. Therefore, while these probes are commonly used, many precautionary steps must be taken to ensure proper detection of thiols with minimal noise. In many cases, these probes should also be validated against proven methods (HPLC, MS) for thiol detection since there is currently very little data available on these newly available dyes.

2B.5 - Thiol Redox State Detection with DIGE

We have mentioned a number of tools that are currently available to researchers who are interested in measuring the redox state of cells and proteins. An important consideration to make

when discussing measurement of thiol redox states is whether we want to measure the reduced state or the oxidized state of proteins or cells. While probes are available for the detection of either form of modification, it may be more efficient for a researcher to choose one. In their study of measuring vicinal dithiols within mitochondria, Murphy et al. have proposed that measuring oxidation is more sensitive using the Redox difference in gel electrophoresis (DIGE) method⁷⁹. In brief, this procedure incubates samples with N-ethylmaleimide (NEM) to irreversibly block reduced thiols in their reduced state. The entire sample is then incubated with the reducing agent dithiothreitol (DTT) to reversibly reduce any remaining oxidized thiols and the sample is then incubated with a fluorescent maleimide-based dye specific to reduced thiols (Cy5)⁷⁹ prior to detection. This method essentially measures samples that were originally in the oxidized state. The major limitation to this DIGE method is that it relies on reversible oxidation of thiols and does not account for many irreversible forms of oxidation that may occur. Furthermore, while it is claimed that this method is more sensitive than measuring reduced states of thiols, the report fails to make a comparison to the latter in order to validate this. Currently, it is still unclear whether measurement of reduction or oxidation will yield more sensitive results. While oxidation can lead to many products, reduction of thiols has the potential of being more simple and sensitive for determining shifts in protein redox state.

2C - Barriers to simplified detection of cellular redox state in tissue lysate

As noted above, while a variety of approaches are being developed or are in use to detect oxidation-specific products on protein thiols, there are many cases where thiol redox state is required regardless of the oxidation product. Thus, in order to determine whether a protein is oxidized in any form, or reduced, it is clear that direct detection of thiol redox state would be

superior to indirect methods (e.g. GSH/GSSG). The availability of several maleimide-based fluorophores for labeling reduced cysteines has made it possible to detect protein redox state with gel electrophoresis. As discussed above, in-gel detection offers a considerable advantage over mass spectrometry given the widespread availability and low cost of electrophoresis infrastructure and expertise. However, the sensitivities of the fluorophores themselves have not consistently been reported⁷⁹ which makes it challenging to select an ideal probe for protein labeling based on the available literature, and not all validations have comprehensively validated the dyes with both oxidation and reduction challenges in vitro and in vivo^{26,79-81}. Furthermore, anecdotal feedback from many investigators (unpublished) indicates that the assays are difficult to establish or signals are too weak to detect in mixed protein lysates. This may be related to the use of poorly binding or insensitive probes. For example, many of these probes often require saturating concentrations of probe that may result in poor protein yields given labeled proteins tend to precipitate⁸⁰. Furthermore, unpublished findings from our lab has noted the considerable variability of results that can be attributed to various experimental assay parameters such as diverse effects of detergents, which has also been reported by one group with certain fluorophores⁸⁰, poor fluorescent signals in protein-rich lysates and generally weak signals in dyes fluorescing in the visual wavelength. There is a clear need to resolving multiple experimental parameters in order to provide a simplified and sensitive method for direct-detection of protein redox state that can be easily and affordably adopted by laboratories with common gel electrophoreses infrastructure.

Chapter 3: Purpose

The purpose of this thesis was to resolve a series of technical limitations to direct detection of cysteine redox state of proteins from muscle tissue lysates using common mini-gel electrophoresis infrastructure. We employed a recently developed infrared fluorescent-tagged maleimide (IRDye 800CW Maleimide, Licor) given infrared fluorescence is known to provide less background and greater sensitivity than visual wavelength fluorescence. This thesis also aimed to resolve a number of experimental barriers that our lab has identified (unpublished) to prohibit detection of thiol redox state using gel electrophoresis. A simplified protocol is then provided which addresses how thiol labeling with IRDye 800CW Maleimide is affected by a common cell lysate detergent, the presence of endogenous low molecular weight compounds and the effect of pH on common reducing controls. We also determined whether oxidation/reduction challenges create homogeneous or heterogeneous responses throughout the redox proteome between 25-100kDa in comparison to a single ‘whole-cell’ assessment using in-well detection. Finally, the in-gel approach of detecting thiol reduction was compared to the reverse DIGE method of quantifying thiol oxidation in order to determine which method is more sensitive at capturing changes in redox state in response to oxidation/reduction challenges. These results were also compared to the more common but indirect assessments of protein oxidation (GSH/GSSG and carbonylation).

Chapter 4: Methods

Sample preparation and treatment

Sprague Dawley heart was harvested, rinsed with 0.9% saline and immediately frozen in liquid nitrogen. Frozen tissue was chipped in liquid nitrogen and homogenized in a plastic microcentrifuge tube with a tapered Teflon pestle in ice cold Tris Buffer (144.5mM Tris, 1.44mM MgCl₂, pH 7.1) containing protease inhibitor cocktails and phosphatase inhibitors (Sigma, St. Louis, MO, cat #: P0044, P5726). Supernatants were obtained by centrifugation at 13,500 rpm for 10 minutes at 4^oC and separated into 130µl aliquots. Each aliquot was spun twice consecutively through a Zeba desalting column (Pierce, Rockford, IL, cat # 89882) with a filtration size of 7kDa. Protein concentration was determined using the bicinchoninic acid (BCA) assay kit (Pierce, Rockford, IL, cat # 23227) and each sample was diluted to equal protein concentration and volume. This was followed by incubation with either 5mM dithiothreitol (DTT) (Bioshop, Burlington, ON, DTT002.5) 1mM tris (2-carboxyethyl) phosphine) (TCEP; Pierce, Rockford, IL, 20490) as thiol reduction controls or 5mM H₂O₂ (Sigma, St. Louis, MO, 323381) containing 0.5% sodium iodide (NaI) (Sigma, St. Louis, MO, 217307) as oxidation controls for 5 minutes at room temperature on a rotating nutator. From this point on, all samples were protected from light as much as possible to prevent the breakdown of any light-sensitive reagents such as IRDye800CW-Maleimide, TCEP, DTT, H₂O₂ and NaI. Some samples that were treated with 5mM H₂O₂ + NaI were subsequently treated with TCEP to see reversible effects of reduction on pre-oxidized samples. These 'rescue' conditions were treated with the same 5mM of H₂O₂+NaI, desalted through Zeba columns to filter small molecules below 7kDa to remove excess reagents and then treated with 1mM TCEP before continuing with the next steps.

After incubation, all samples were desalted twice using Zeba columns which retain anything at or below 7kDa to remove excess reagents. The protein concentration of each sample was then determined using another BCA protein assay. For experiments using reducing agents such as DTT and TCEP, a reducing agent-compatible BCA kit was used (Pierce, Rockford, IL, cat#23252). Once protein content was determined, samples were diluted to equal volumes and protein concentrations. IRDye800CW-Maleimide was then added at a ratio of 400 μ M for every 200 μ g of protein. Samples were incubated with dye overnight at 4°C on a rotating nutator. The following day samples were desalted a final time to remove excess dye prior to preparation for western blotting.

Western Blotting and in-well assays

Another BCA protein assay was conducted to prepare equal proteins for western blotting samples. For all western blots, 2 μ g of protein was loaded per lane on polyacrylamide running gels of 10% and subjected to SDS-PAGE at 160 volts for 75 minutes until the blue front from the laemelli's reagent ran off the bottom of the gel. Gels were detected at emission wavelengths of at 800nm and 700nm fluorescent wavelengths for the dye and protein standard (Bio-Rad, Mississauga, ON, 161-10374) respectively using the Odyssey infrared imaging system (Licor Biosciences, Lincoln, NE, Model # 9120). All gels were scanned at an intensity unit of 5 for both 800 and 700nm channels

Similarly for the in-well assays using 96-well plates, 2 μ g of each sample was loaded into a well and topped up to a final volume of 200 μ l per well with double distilled water (ddH₂O). The well was then scanned on the Odyssey imaging system using a lower intensity unit of 2 to eliminate background and plate reflection. In order to determine any background interactions between IRDye800CW-Maleimide and other reagents (TCEP, H₂O₂+NaI), separate wells were

loaded with either ddH₂O, 1mM TCEP or 5mM H₂O₂+NaI with 100nM IRDye800CW-Maleimide and brought to a final volume of 200µl.

Heat treatment

Given that heat is known to alter the redox state of cellular proteins^{25,82-84}, we used this model to trigger altered redox states in our samples. Frozen cardiac muscle was placed in solution containing (mM): NaCl, 145; KCl, 3; CaCl₂, 2.5; MgCl₂, 1 and Hepes, 10 with a final pH of 7.4. This buffer was pre-heated to either 40⁰C or 49⁰C in a dry bath incubator prior to addition of frozen tissue while controls remained at room temperature. Following 45 minutes incubation at their respective temperatures, control and heated samples were removed, quickly blotted dry and placed in Tris buffer containing protease and phosphatase inhibitors for homogenizing following the steps outlined previously.

Redox-DIGE

Heated samples subjected to our optimized and direct redox protocol were compared to a modified redox method by Murphy et al.⁷⁹. In this difference in gel electrophoresis (DIGE) method, heated samples were incubated with 50mM N-ethylmaleimide (NEM) (Sigma, St. Louis, MO, E3876) followed by two consecutive washes through Zeba columns to remove excess NEM. Samples were then reduced with 2mM TCEP and desalted again to remove excess TCEP. Protein concentration was then determined and samples were diluted to equal volumes and protein concentrations followed by an overnight incubation with IRDye800CW-Maleimide at 4⁰C. Western blotting procedures outlined above were then conducted the next day.

GSH and GSSG measurements using HPLC

Tissue was homogenized in Tris buffer containing (mM): 50 Tris, 20 boric acid, 2 L-serine, 20 acivicin and 5 NEM at a pH of 8. To deproteinate our samples, trichloroacetic acid was added to homogenate for GSH, and perchloric acid was used for GSSG. Deproteinated samples were vortexed vigorously and centrifuged at 14,000 RPM for 5 minutes at 4°C. Supernatants were collected and sampled through a High-Pressure Liquid Chromatography (HPLC) system (Agilent, Santa Clara, CA, 1100 Series) equipped with a 4.6 x 150 mm, 5-micron column (ZORBAX Eclipse XDB-C18, Agilent, Santa Clara, CA). GSH measurements were taken using ultraviolet emissions picked up by the variable wavelength detector. The mobile phase for GSH was 0.25% glacial acetic acid in HPLC-grade water, flow rate of 1.25 ml/min (pH 3.1). For GSSG analysis, 200 µl of supernatant was added to 1 ml of 0.5 M NaOH followed by a 15 minute light-protected incubation with 75 µl 0.1% o-Pthaldialdehyde (OPA), a fluorescent probe. Mobile phase for GSSG separation was sodium phosphate dibasic. Eluted GSSG was directed to a high resolution fluorometer (QuantaMaster 40, HORIBA Scientific, Edison, New Jersey) in a high pressure flow-through cuvette (Firefly Sci, Brooklyn, NY, 8830). GSSG mobile phase consisted of sodium phosphate dibasic, flow rate of 0.5 ml/min. Using GSH and GSSG standard curves, both GSH and GSSG were expressed as µmol/g protein.

Carbonylation

All procedures for derivitization of protein carbonyls with 2,4-dinitrophenylhydrazine (DNPH) were conducted using the Oxy blot kit (S7150, Millipore, Etobicoke, ON). Briefly, carbonyl products react with DNPH to form 2,4-dinitrophenylhydrazone (DNP-hydrazone) which is subsequently measured using chemiluminescence. 15 µg of protein was loaded from heated (40°C or 49°C) and control heart muscles from Sprague Dawley rats. Proteins were

denatured with 12% SDS followed by derivatization (DNPH solution or control) for 20min with gentle agitation at room temperature. The derivatization reaction was stopped with the addition of neutralization solution and samples were reduced with 2-mercaptoethanol (5% v/v). Proteins were separated on a 12% polyacrylamide gel and transferred onto a polyvinylidene fluoride (PVDF) membrane. Membranes were blocked in odyssey blocking buffer for 1 hour prior to overnight incubation with primary antibody (1:150, Rabbit Anti-DNP). On the following day membranes were washed with TBST and incubated with goat anti-rabbit IgG 680 (Licor, 926-68071) for 1 hour and imaged (Odyssey, Licor Bioscience).

Data Analysis and statistics

Densitometry of fluorescence was quantified for all western blots and microwell plate analyses using the Licor Odyssey software version 2.0.13. Lanes were selected between 25-100kDa while specific bands at 60kDa, 44kDa and 25kDa were individually assessed to determine their influence on whole-lane fluorescence. For in-well images, the entire well was selected for quantification of fluorescence densitometry values. Gel data comparing control, oxidized (5mM H₂O₂+NaI) and rescued (sequential 5mM H₂O₂+NaI oxidation with 1mM TCEP reduction) conditions was analyzed using a Friedman's non-parametric test. Plate data comparing the same conditions passed the Kolmogorov-Smirnov test for normality and was analyzed using a one-way ANOVA with repeated measures. The Student Newman-Keuls post hoc test was used to identify which means were significantly different from each other. Results are expressed as mean ±SEM. Significance for all stats was established at P<0.05. All data comparing only 2 groups were analyzed using a paired two-tailed t-test.

Chapter 5: Results

Prior to obtaining the results outlined in this section, a number of important optimization steps had to be performed in order to determine the appropriate conditions for the IRDye800CW Maleimide to accurately detect reduced thiols. Most of these steps are outlined in the appendix while some are shown in this section.

Effects of Desalting Samples Prior to Dye Treatment

Filtering homogenates through a desalting column prior to incubating with IRDye800CW Maleimide resulted in an increased signal in these desalted (D) conditions compared to no desalting (ND). This observation was found to occur in gel for both CHAPS buffer (ND: 1.93 ± 0.21 a.u., D: 35.63 ± 2.44 a.u., $p < 0.05$) and Tris buffer (ND: 1.28 ± 0.39 a.u., D: 33.34 ± 4.39 a.u., $p < 0.05$, Figure 4a). Similar results were observed using an in-well approach in CHAPS (ND: 1.43 ± 0.18 a.u., D: 12.66 ± 0.51 a.u., $p < 0.05$) and Tris (ND: 2.56 ± 0.39 a.u., D: 11.89 ± 1.79 a.u., $p < 0.05$, Figure 4c). Desalting also led to a decrease in GSH content (2.92 ± 0.07 $\mu\text{mol/g}$, $p < 0.05$) compared to non-desalted controls (3.35 ± 0.09 $\mu\text{mol/g}$, $p < 0.05$, Figure 5). After determining that desalting prior to dye incubations greatly enhances our fluorescent signal, we proceeded to incorporate this important step in our remaining experiments for all treatment conditions that would be subjected to IRDye800CW Maleimide incubations.

Effects of Desalting Prior to Dye Labeling

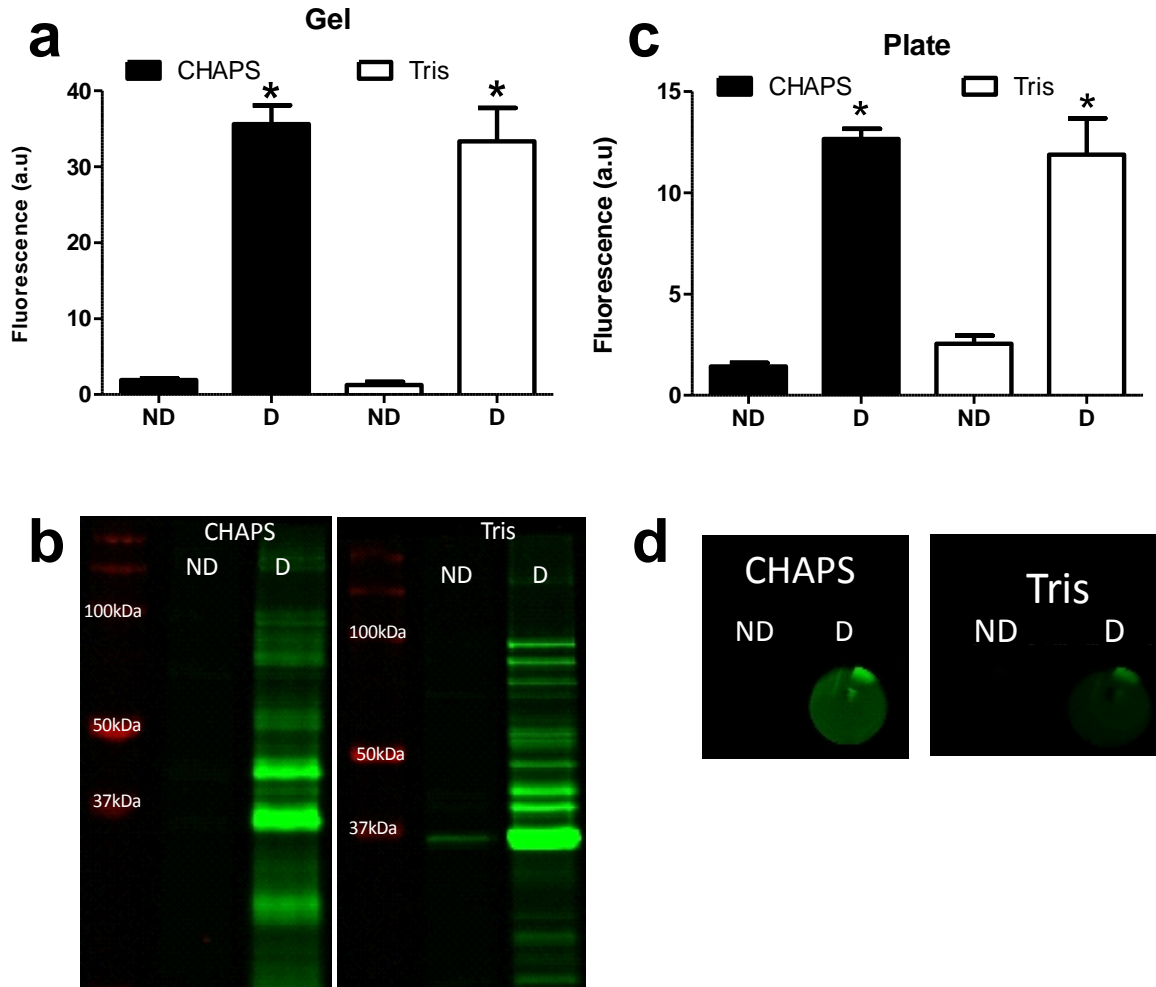


Figure 4. Effects of desalting homogenates prior to dye treatment in gel (a and b) and in plate (c and d). Desalted samples (D) showed much greater fluorescence compared to non-desalted (ND) samples in both CHAPS (pH 7.5) and Tris (pH 7.1). Results represented as mean \pm SEM. N=4-6. * indicates significant difference from ND, $p < 0.05$.

Effects of Desalting on GSH Content

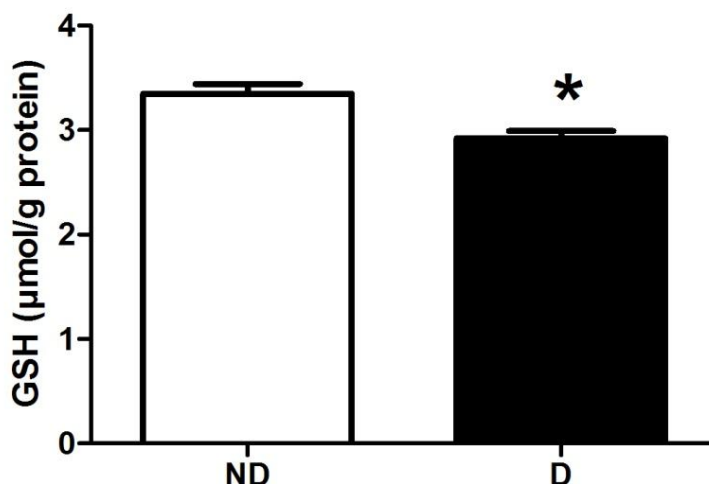


Figure 5. Effects of desalting on GSH content. The desalted condition (D) led to a significant decrease in GSH content of homogenates when compared to the non-desalted (ND) condition. Results represent mean \pm SEM. N=6. * indicates significantly different from ND, $p < 0.05$.

Quenching Effects of Reagents on IRDye800CW Maleimide

In order to determine the interactions between oxidizing ($\text{H}_2\text{O}_2 + \text{NaI}$) and reducing (TCEP) agents with IRDye800CW Maleimide, we performed a test to determine whether quenching of fluorescence occurred in the presence of these reagents. There was a significant decrease in fluorescence between $\text{H}_2\text{O}_2 + \text{NaI}$ and TCEP in dye compared to the dye alone (IRDye: 282.4 ± 40.54 a.u., IRDye + OX: 228.06 ± 38.76 a.u., $p < 0.05$, IRDye + RED: 224.18 ± 40.8 a.u., $p < 0.05$, Figure 6)

Quenching effects of Oxidizing and Reducing Agents on IRDye800CW Maleimide

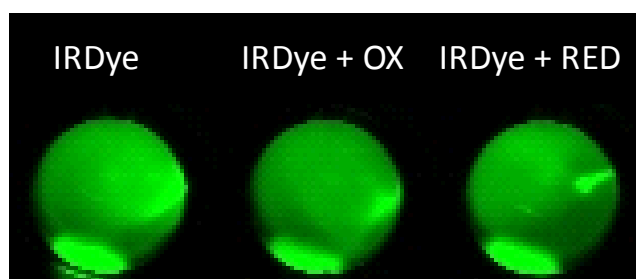
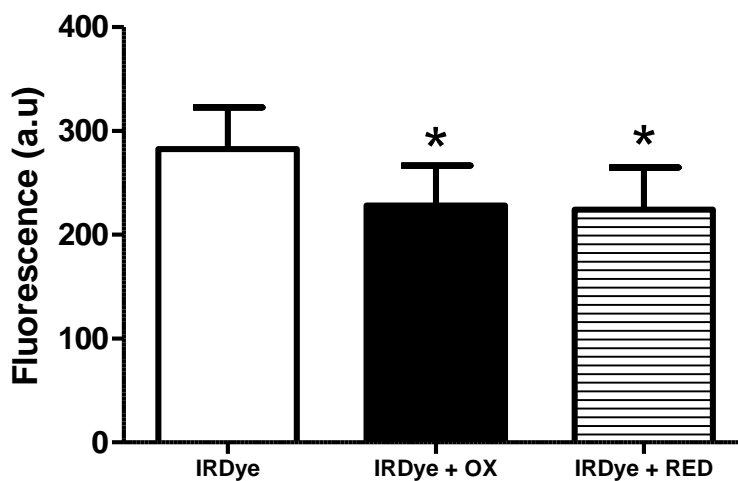


Figure 6. Quenching effects of reagents on IRDye800CW Maleimide. The use of 5mM H_2O_2+NaI (OX) or 1mM TCEP (RED) in conjunction with IRDye had a small but significant effect on fluorescence compared to IRDye alone. Results represent mean \pm SEM. N=7. * indicates significantly difference from IRDye

Effects of Oxidizing and Reducing Agents on IRDye800CW Maleimide Fluorescence

After treating separate homogenates with oxidizing (H_2O_2+NaI) and reducing (TCEP) agents, in-gel fluorescence was measured to determine if the dye accurately detects the respective changes in redox states brought about by these reagents. When considering absolute fluorescence values, oxidized samples were significantly lower than controls while reduced samples were not

significantly different from controls (Control: $1.64 \times 10^6 \pm 0.67 \times 10^6$ a.u, Oxidized: $0.027 \times 10^6 \pm 0.01 \times 10^6$ a.u, $p < 0.05$, Reduced: $1.11 \times 10^6 \pm 0.49 \times 10^6$ a.u, Figure 7).

Effects of Oxidizing and Reducing agents on IRDye800CW Maleimide in-Gel Fluorescence

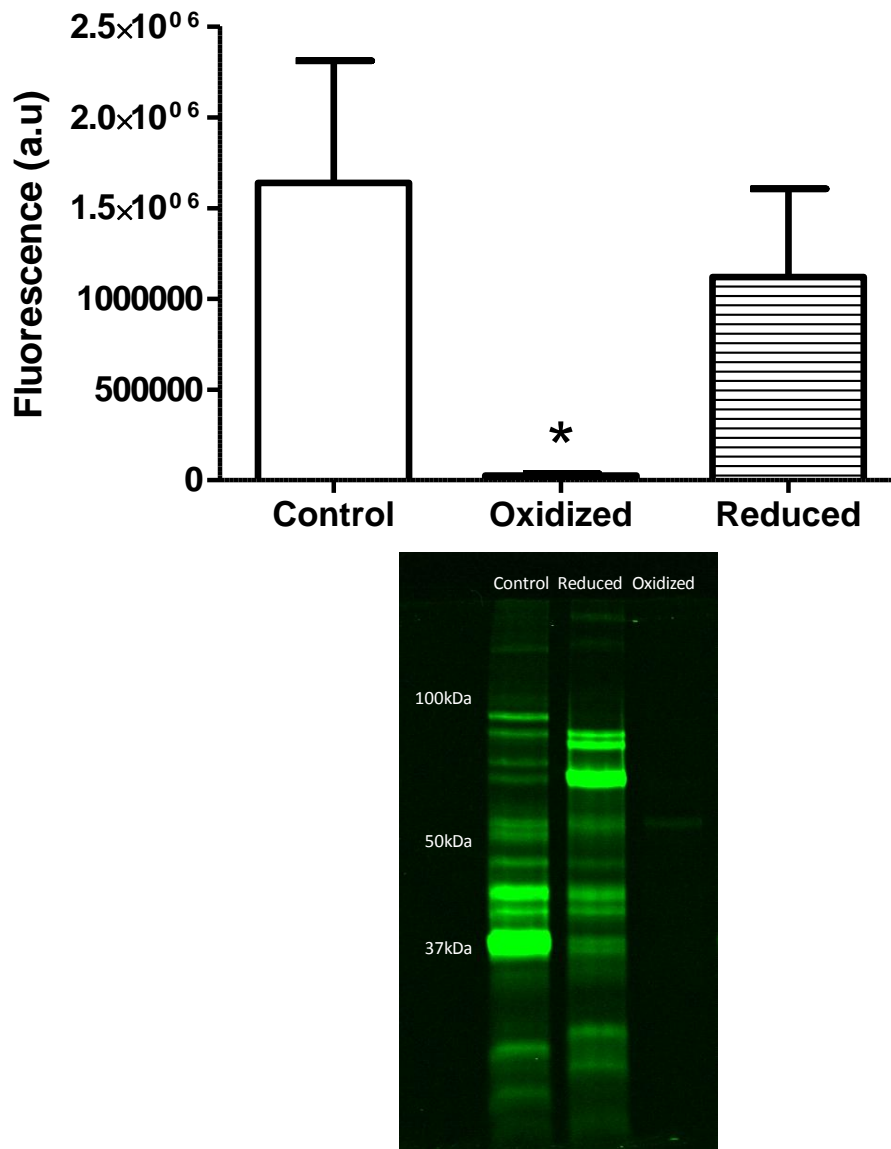


Figure 7. Effects of reducing and oxidizing samples on IRDye800CW Maleimide in-gel. Only oxidized samples were significantly different than controls while reduced samples showed a trending yet insignificant decrease. Results represented as mean \pm SEM. * indicates significant difference from control, $p < 0.05$. N=6.

Rescuing Effects of oxidized samples with TCEP

We proceeded to test the 'rescuing' effects TCEP would have on samples that had been pre-treated with $\text{H}_2\text{O}_2 + \text{NaI}$ in order to determine its efficacy as a reducing agent. Using IRDye800CW Maleimide in an in-gel approach showed that the oxidized group was significantly lower than control fluorescence while the rescue condition showed no difference (Control: 107.48 ± 4.71 a.u., Oxidized: 3.29 ± 1.21 a.u., $p < 0.05$, Rescued: 100.82 ± 20.77 a.u., Figure 8a). With the in-gel approach, a significant decrease in fluorescence was observed in the reduced conditions when normalized to control (Reduced: 0.77 ± 0.03 a.u., $p < 0.05$, Figure 8b inset) however this difference was abolished when comparing absolute fluorescent values (Reduced: 70.18 ± 11.51 a.u., Figure 8b). Using the plate approach, oxidized samples were significantly lower than control and rescued conditions (Control: 6.27 ± 1.14 a.u., Oxidized: 0.098 ± 0.024 a.u., Rescued: 6.68 ± 1.02 a.u., Figure 9a). When compared to control, reduced samples showed significantly greater fluorescence when (Reduced: 7.54 ± 1.28 a.u., $P < 0.05$, Figure 9b).

We also determined the GSH and GSSG content as well as the ratio of GSH/GSSG to determine the repeatability of results obtained through in-gel and plate approaches. We found no significant difference in GSH content between control, oxidized and rescued conditions (Control: 30.55 ± 2.33 $\mu\text{mol/g}$, Oxidized: 31.39 ± 2.91 $\mu\text{mol/g}$, Rescued: 31.61 ± 1.71 $\mu\text{mol/g}$, Figure 10-a1). Similarly, no differences were found between control and reduced conditions in GSH content (Reduced: 30.71 ± 1.67 $\mu\text{mol/g}$, Figure 10-a2). GSSG content showed no difference between control, rescued and reduced conditions, however the GSSG content of oxidized samples was elevated (Control: 1.1 ± 0.095 $\mu\text{mol/g}$, Oxidized: 1.55 ± 0.18 $\mu\text{mol/g}$, Rescued: 1.22 ± 0.11 $\mu\text{mol/g}$, Reduced: 1.07 ± 0.09 $\mu\text{mol/g}$, Figure 10-b1 and b2). The ratio of GSH/GSSG

showed no differences between groups (Control: $27.48 \pm 3.4 \mu\text{mol/g}$, Oxidized: 21.36 ± 2.69 , Rescued: 26.64 ± 1.73 , Reduced: 28.1 ± 2.11 , Figure 10-c1 and c2).

Rescue Effects of TCEP on Pre-Oxidized Samples (Gel)

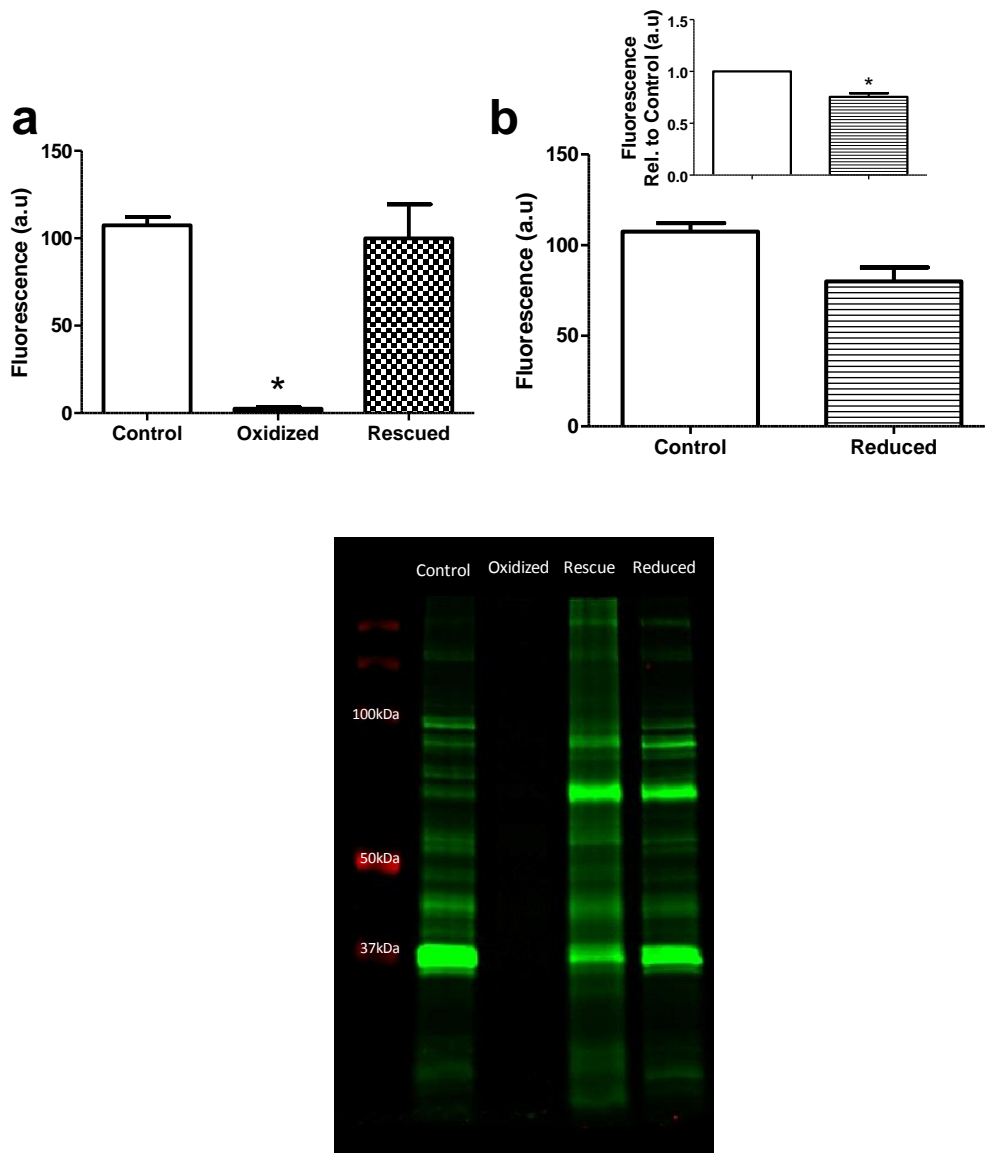


Figure 8. Rescue effects of TCEP on pre-oxidized samples using in-gel approach. In the rescue condition, samples were first oxidized with $\text{H}_2\text{O}_2 + \text{NaI}$ and then treated with TCEP. This returned fluorescence of oxidized samples back to control and reduced levels (a) with the same statistical findings relative to control (graph not

shown). No significance was found between control and reduced samples (b) however when considering fluorescence relative to control, reduced samples showed a significant decrease (b. inset) Results represented as mean \pm SEM. N=4-6. * indicates significantly different from Control, $p < 0.05$.

Rescue Effects of TCEP on Pre-Oxidized Samples (Plate)

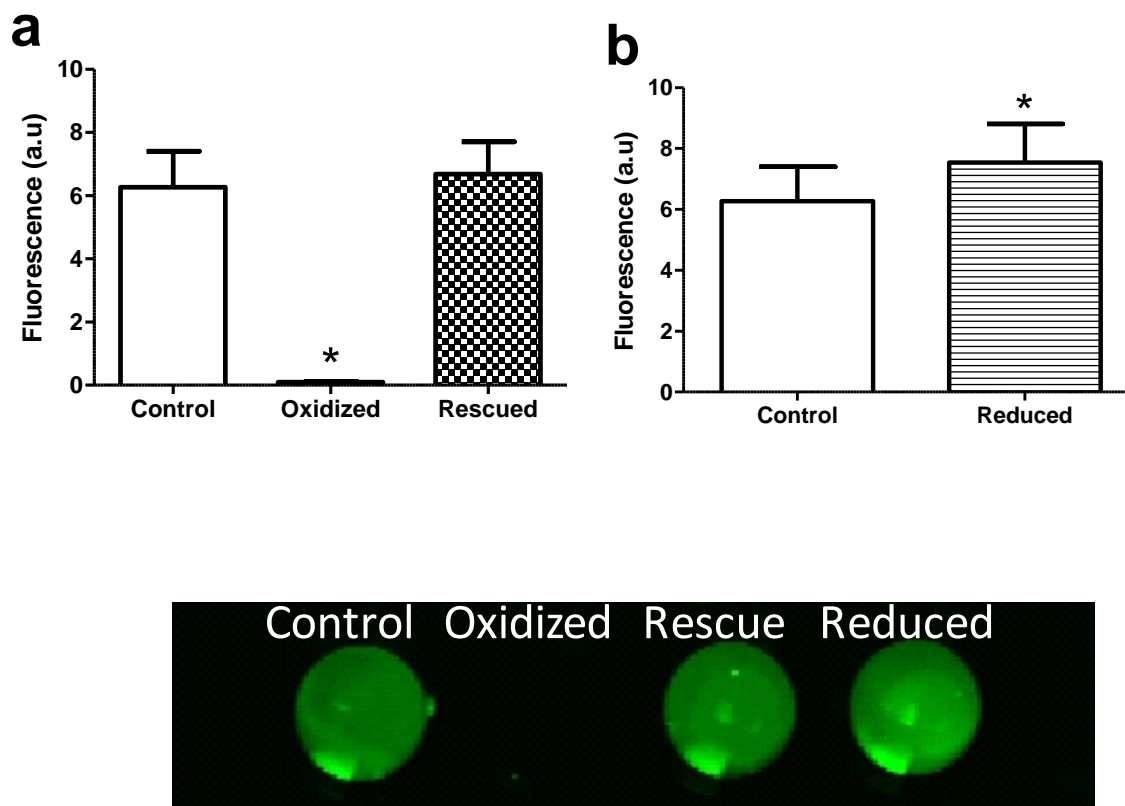


Figure 9. Rescue effects of TCEP on pre-oxidized samples using in-well approach. In the rescue condition, samples were first oxidized with H_2O_2+NaI and then treated with TCEP. This returned fluorescence of oxidized samples back to control (a) The reduced condition showed greater fluorescence compared to (b). Results represented as mean \pm SEM. N=6. * indicates significantly different from Control, $p < 0.05$.

Rescue Effects of TCEP on GSH and GSSG Content

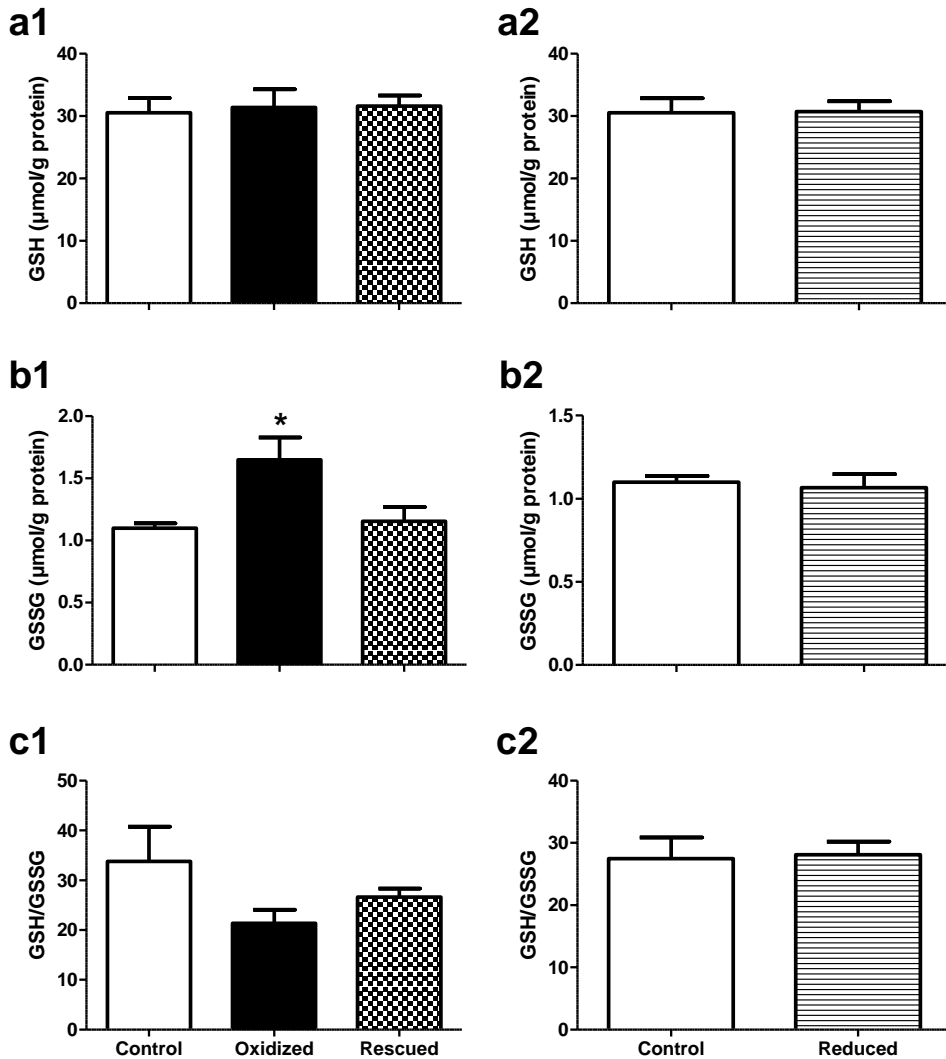


Figure 10. Effects of reducing and oxidizing agents on GSH, GSSG and GSH/GSSG. No difference was observed in GSH content (a), GSSG (b) or GSH/GSSG (c) however there is a trending increase in GSSG for oxidized samples (b1) and a trending decrease in their GSH/GSSG ratio (c1). Results represented as mean \pm SEM. N=5-6.

Heat-induced changes in redox states

49°C Treatment

With respect to the direct detection of reduced thiols using our optimized protocol with IRDye800CW Maleimide, exposure of tissue samples to 49°C temperatures led to a significant decrease in fluorescence in the 25-100kDa range using the in-gel approach relative to control (49°C: 0.315 ± 0.07 a.u, $p < 0.05$, Figure 11e inset) with similar findings using absolute fluorescence (Control: 50.15 ± 7.21 a.u, 49°C: 16.67 ± 4.44 a.u, $p < 0.05$, Figure 11e). No difference was found after 49°C treatment for the 25kDa, 44kDa and 60kDa bands (25kDa Control: 0.67 ± 0.12 a.u, 25kDa 49°C: 0.91 ± 0.35 a.u, 44kDa Control: 4.29 ± 0.4 a.u, 44kDa 49°C: 4.73 ± 1.49 a.u, 60kDa Control: 0.6 ± 0.07 a.u, 60kDa 49°C: 1.02 ± 0.24 a.u, Figure 11b, 11c and 11d, respectively).

Using the plate approach for 49°C treated samples, we found that heated samples had significantly lower fluorescence compared to controls (Control: 2.56 ± 0.38 a.u, 49°C: 0.58 ± 0.22 a.u, $p < 0.05$, Figure 12).

The GSH content of 49°C treated samples did not differ from control (Control 18.41 ± 4.07 $\mu\text{mol/g}$, 49°C: 18.71 ± 2.51 $\mu\text{mol/g}$, Figure 13a). GSSG content was significantly greater in the heat treated group (Control: 1.31 ± 1.68 $\mu\text{mol/g}$, 49°C: 2.15 ± 0.17 $\mu\text{mol/g}$, $p < 0.05$, Figure 13b) while the ratio of GSH/GSSG showed a significant decrease after heating at 49°C (Control: 13.39 ± 1.68 , 49°C: 8.35 ± 0.63 , $p < 0.05$, Figure 13c).

Effects of 49°C Treatment on IRDye800CW Maleimide Fluorescence in Gel

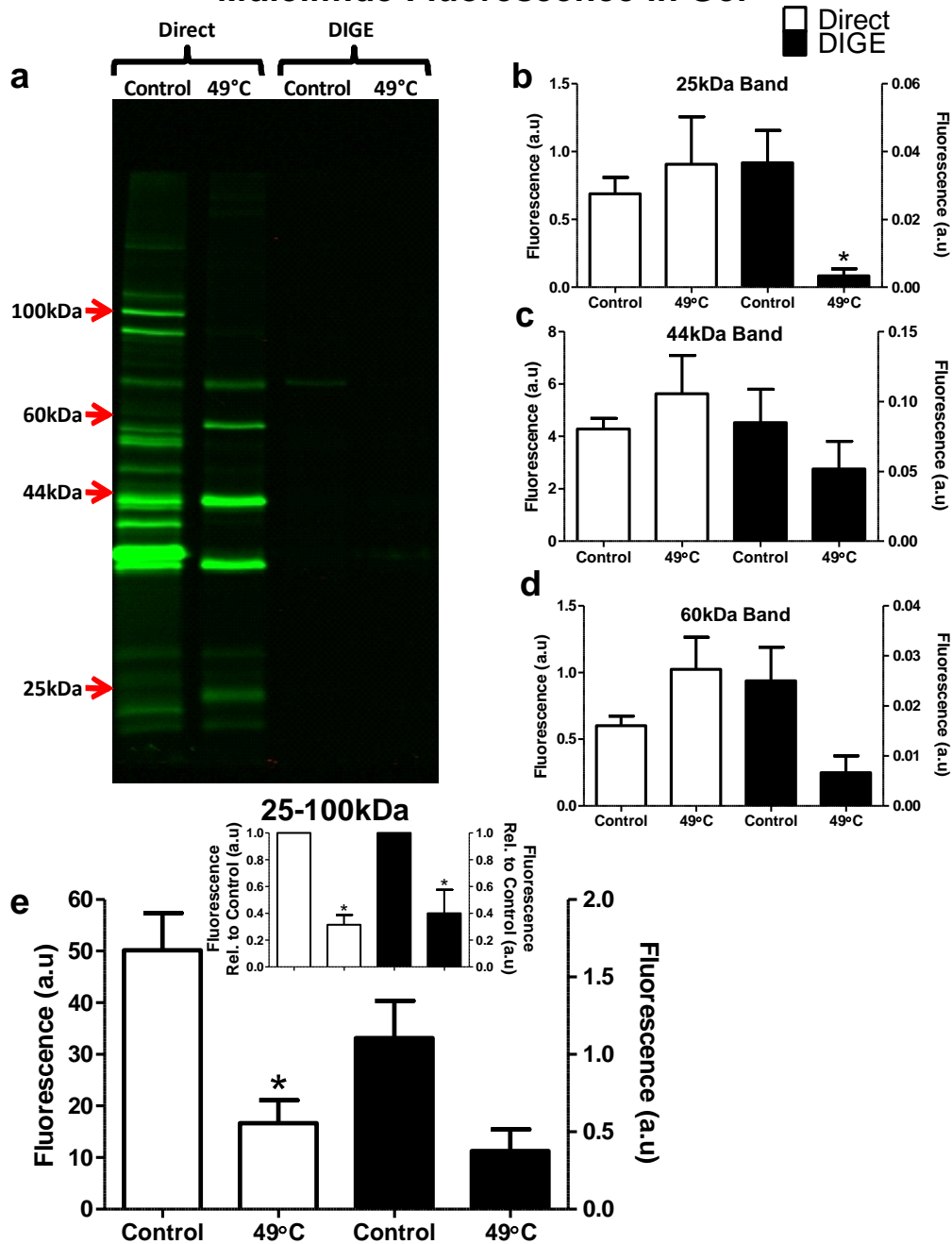


Figure 11. Effects of 49°C heat treatment on fluorescence using in-gel approach. Using the direct redox method, 49°C significantly decreased fluorescence between 25-100kDa for both absolute (e) and relative (e. inset) values. This difference was removed when bands at 25kDa, 44kDa and 60kDa (b, c and d, respectively) were considered. Signals from these bands in the heated condition trended higher than controls. DIGE results showed no difference after heating with absolute fluorescence

densitometry (e) however there was a significant decrease after heating relative to control fluorescence (e. inset). All other panels showed similar statistics with absolute and normalized values (data not shown). Results represented as mean \pm SEM. * indicates significantly different from control, $p < 0.05$. $N = 5-6$.

Effects of 49°C Treatment on IRDye800CW Maleimide Fluorescence in Plate

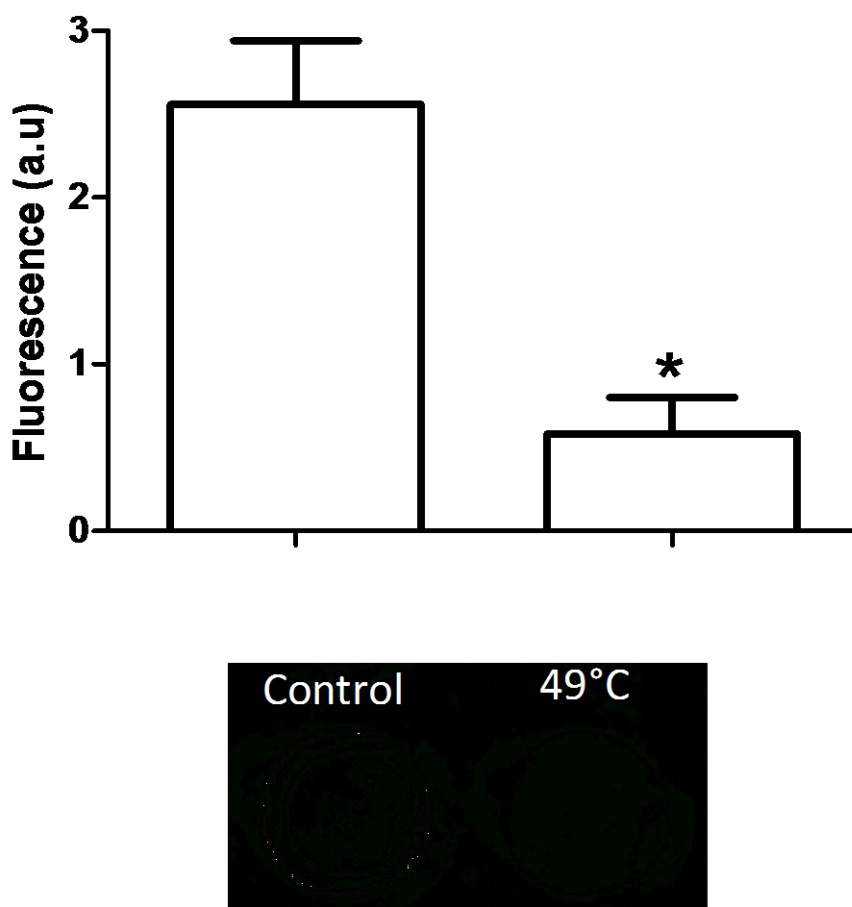


Figure 12. Effects of 49°C heat treatment on fluorescence using in-well plate assay. Samples exposed to 49°C temperatures showed a decrease in fluorescence compared to control. Results represented as mean \pm SEM. * indicates significantly different from control, $p < 0.05$. $N = 5$.

Effects of 49°C Treatment on GSH and GSSG Content

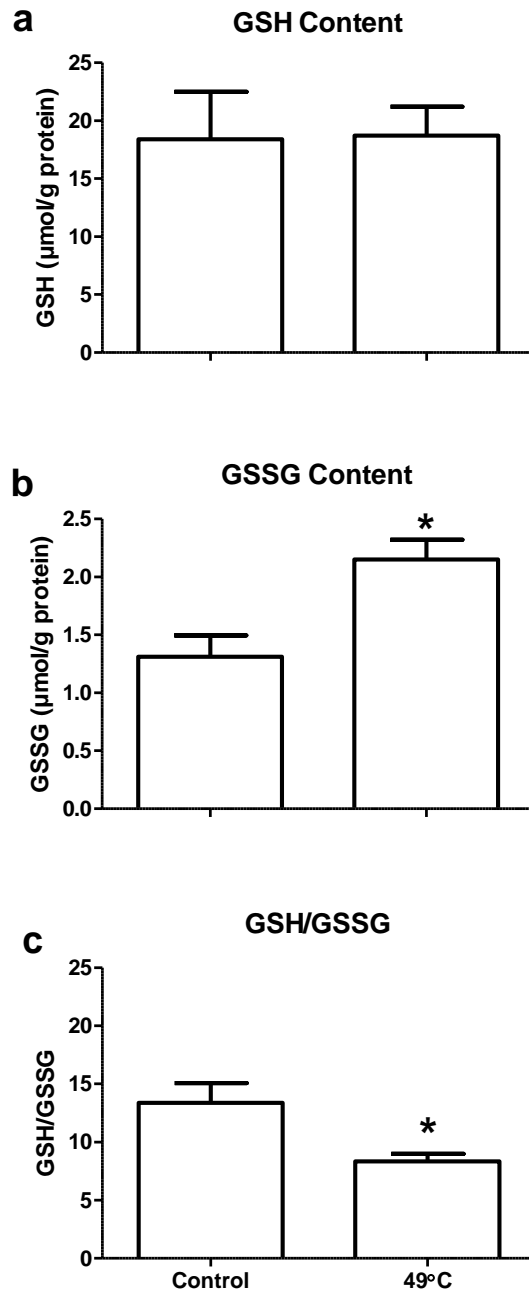


Figure 13. Effects of 49°C heat treatment on GSH, GSSG and GSH/GSSG ratio. Samples exposed to 49°C temperatures showed no significant change in GSH content (a) while GSSG content significantly increased (b) and GSH/GSSG ratio significantly decreased (c). Results represented as mean \pm SEM. * indicates significantly different from control, $p < 0.05$. N=4-5.

40°C Treatment

In contrast to 49°C incubations, 40°C incubations showed no significant difference in fluorescence with the in-gel assay using our direct method (Control: 37.21 ± 0.89 a.u, 40°C: 31.23 ± 11.52 a.u, Figure 14e) with the same statistical findings when normalized to control (Figure 14e inset). Similarly, no difference was found for the 25kDa, 44kDa and 60kDa bands (25kDa Control: 1.81 ± 0.29 a.u, 25kDa 40°C: 2.19 ± 0.64 a.u, 44kDa Control: 3.96 ± 0.3 a.u, 44kDa 40°C: 4.13 ± 1.22 a.u, 60kDa Control: 0.71 ± 0.04 a.u, 60kDa 40°C: 0.77 ± 0.15 a.u, insets of Figure 14b, 14c and 14d, respectively).

While the DIGE results from 25-100kDa showed no significance when considering absolute values (Control: 11.23 ± 4.18 a.u, 40°C: 1.41 ± 0.48 a.u, Figure 14e), there was a significant decrease in fluorescence using this method when considering values normalized to control (40°C: 0.17 ± 0.05 a.u, $p < 0.05$, Figure 11e inset). Differences were also found after 40°C treatment for the 25kDa, 44kDa and 60kDa bands (25kDa Control: 0.62 ± 0.22 a.u, 25kDa 40°C: 0.05 ± 0.01 a.u, 44kDa Control: 1.7 ± 0.44 a.u, 44kDa 40°C: 0.19 ± 0.05 a.u, 60kDa Control: 0.42 ± 0.11 a.u, 60kDa 40°C: 0.09 ± 0.02 a.u, Figure 14b, 14c and 14d, respectively).

The in-well approach showed no difference compared to control after heating to 40°C (Control: 2.13 ± 0.32 a.u, 40°C: 1.92 ± 0.22 a.u, Figure 15).

These conditions also brought about a significant decrease in GSH content (Control: 16.32 ± 0.41 $\mu\text{mol/g}$, 40°C: 10.15 ± 1.25 $\mu\text{mol/g}$, $p < 0.05$, Figure 16a). GSSG showed no significant change (Control: 0.66 ± 0.02 $\mu\text{mol/g}$, 40°C: 0.74 ± 0.04 $\mu\text{mol/g}$, Figure 16b) while

the GSH/GSSG ratio showed a significant decrease (Control: 24.86 ± 0.38 , 40°C : 13.53 ± 1.09 , $p < 0.05$, Figure 16c).

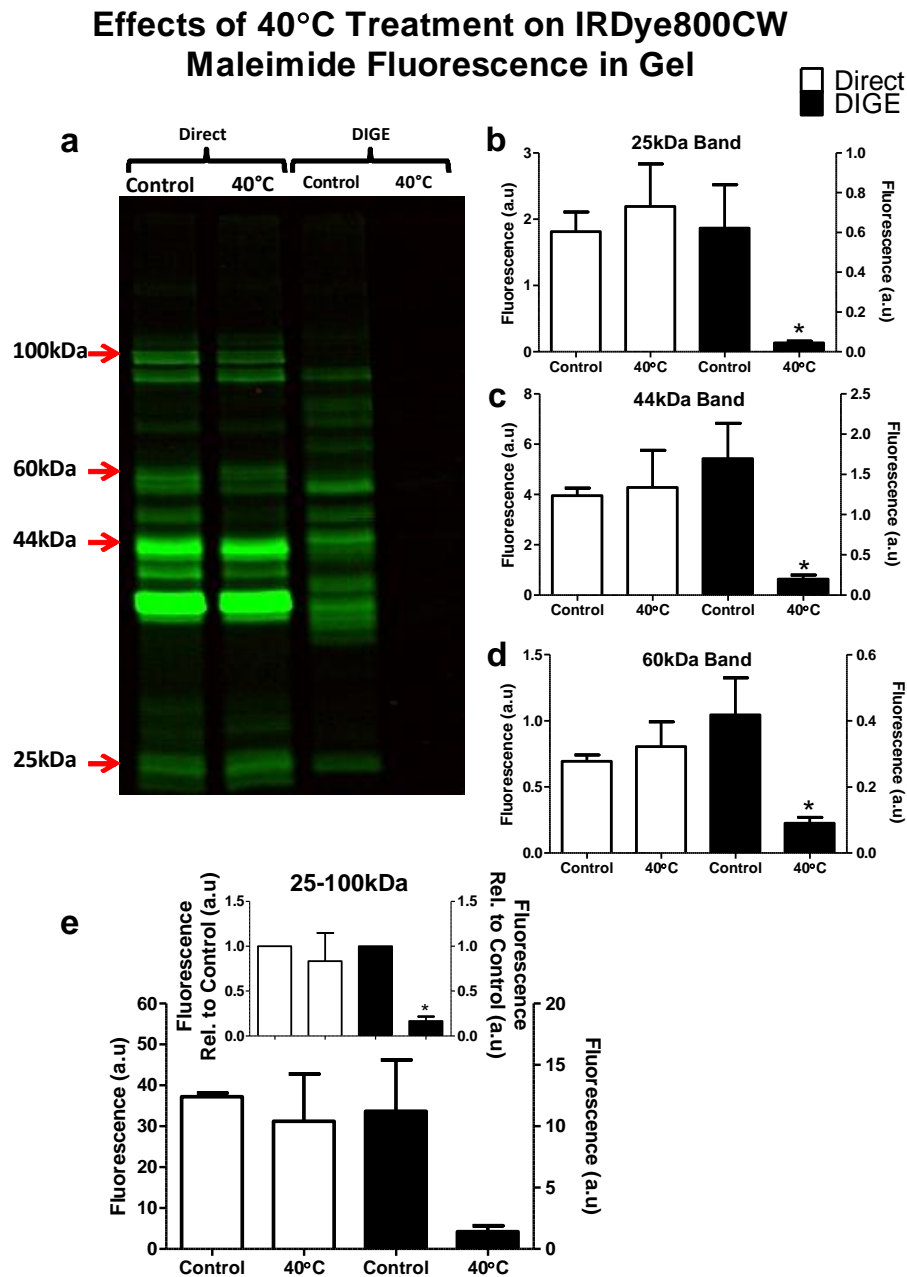


Figure 14. Effects of 40°C heat treatment on fluorescence using in-gel assay. Representative image (a). Using the direct redox method, samples exposed to 40°C temperatures showed no significant change in fluorescence when measuring 25kDa (b), 44kDa (c), 60kDa (d) bands or lane measurements from 25-100kDa (e). The same was found for DIGE results for the individual bands. Our DIGE results at the

25-100kDa range showed no significance after heat treatment when considering absolute fluorescence densitometry (e) however a significantly lower signal was found when normalized to control (e. inset). All other panels showed the same statistical findings with absolute and normalized data (data not shown). Results represented as mean \pm SEM. * indicates significantly different from control, $p < 0.05$. N=5-6. Results represented as mean \pm SEM. * indicates significantly different from control, $p < 0.05$. N=4-6.

Effects of 40°C Treatment on IRDye800CW Maleimide Fluorescence in Plate

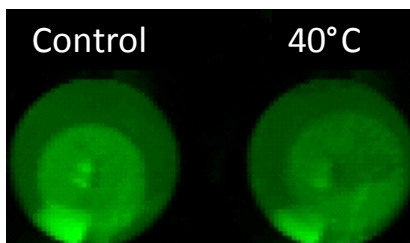
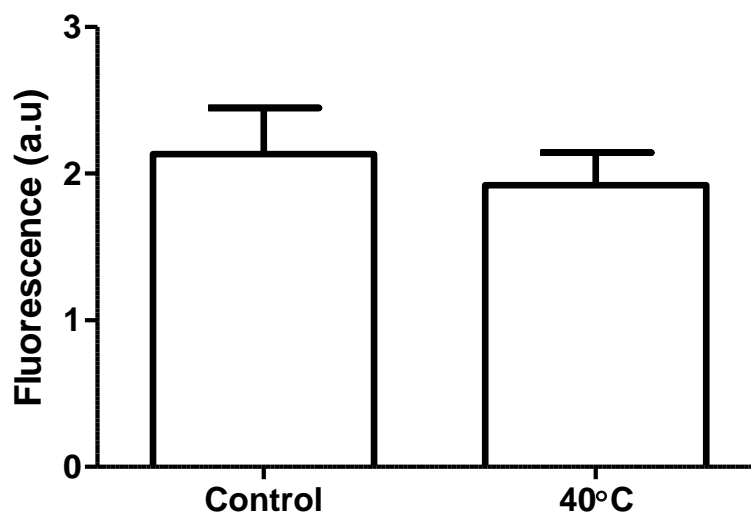


Figure 15. Effects of 40°C heat treatment on fluorescence in-well plate assay. Samples exposed to 40°C temperatures showed no significant change in fluorescence when measured in gel. Results represented as mean \pm SEM. N=6.

Effects of 40°C Treatment on GSH and GSSG Content

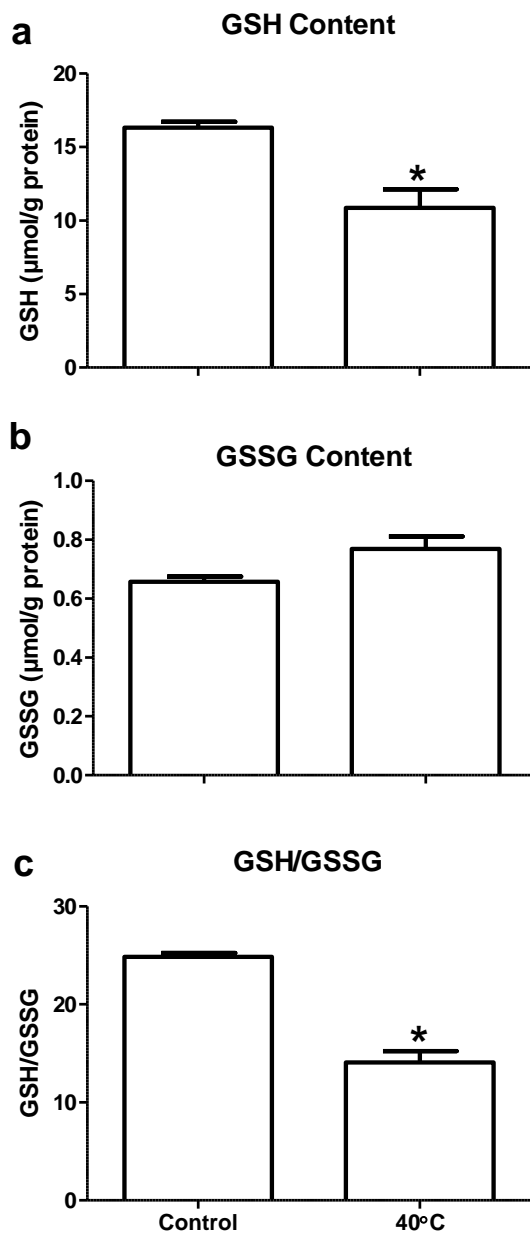


Figure 16. Effects of 40°C heat treatment on GSH, GSSG and GSH/GSSG ratio. Samples exposed to 40°C temperatures showed a significant decrease in GSH content (a) while GSSG content remained unchanged (b). The GSH/GSSG ratio significantly decreased (c). Results represented as mean \pm SEM. * indicates significantly different from control, $p < 0.05$. $N = 5-6$.

Effects of 40°C and 49°C Treatments on Carbonylation

There was no significant change in protein carbonyl products after 40°C (Control: 31.92 ± 3.26 a.u, 40°C: 36.21 ± 3.83 a.u, Figure 17a).

On the other hand, the 49°C treated group showed a significant increase in carbonylation (Control: 33.1 ± 4.13 a.u, 49°C: 93.87 ± 10.23 a.u, $p < 0.05$, Figure 17b).

Effects of 40°C and 49°C Treatment on Protein Carbonylation

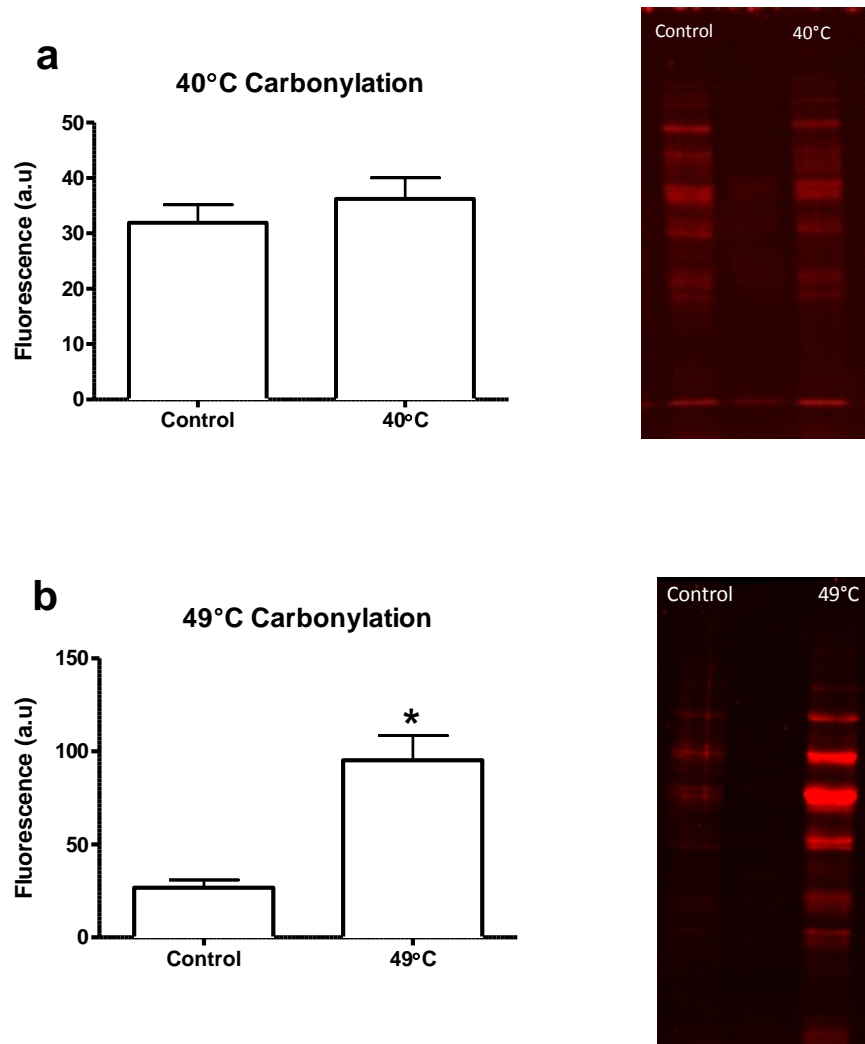


Figure 17. Effects of 40°C and 49°C treatment on protein carbonylation. Heat treatment at 40°C did not show a change in protein carbonylation compared to control (a). 49°C treatment significantly increased the level of carbonylation (b). Results represented as mean \pm SEM. * indicates significantly different from control, $p < 0.05$. N=4-6.

Chapter 6: Discussion

Our aim in this study was to determine whether IRDye800CW Maleimide can accurately detect reduced thiols in cardiac tissue lysates and whole cells using simplified methodologies such as SDS-PAGE and in-well plate assays. In order to do this we first had to establish the appropriate conditions required for the use of IRDye800CW Maleimide. These optimizations are listed in section 6H below. We employed a number of treatments to alter the redox state of lysates in order to confirm the dye's efficacy at accurately detecting reduced thiols through multiple avenues.

6A - Desalting leads to increased fluorescent signal with IRDye800CW Maleimide

Early into our optimization for this assay we noticed that desalting samples through Zeba desalting columns prior to the addition of any reagents led to a large increase in IRDye800CW Maleimide's fluorescence using in-gel and in-well plate assays in both CHAPS and TRIS buffer (Figure 4). We continued our experiments using TRIS since a number of experiments comparing CHAPS and TRIS showed the latter to be more consistent throughout our dye experiments (data not shown). We suspected that endogenous GSH in tissue could be interfering with our dye's ability to bind to protein thiols due to the abundance of GSH in cells (mM range)⁸⁵. Furthermore, we suspected that the Zeba columns, which remove substances below 7000Da were effectively removing endogenous GSH (307Da) thereby allowing more of the dye to bind to the remaining protein thiols leading to an increase in fluorescence. To test this hypothesis we measured GSH content in both non-desalted (ND) and desalted (D) samples. As shown in figure 5, desalting led to a small yet significant drop in GSH content in cardiac tissue lysates. Admittedly, we expected a much larger drop in GSH content after desalting yet our current results suggest that GSH is a

partial contributor to the dye interference we observed and that other factors, such as free cysteine and coenzyme A, may be interfering with dye binding prior to desalting due to the presence of thiols in these molecules.

6B - Oxidizing and reducing agents may interfere with IRDye800CW Maleimide

Next we determined whether our chosen reagents for oxidation ($\text{H}_2\text{O}_2+\text{NaI}$) and reduction (TCEP) would have an interaction with IRDye800CW Maleimide and our results indicate that the dye's fluorescence dropped in the presence of these reagents (Figure 6). It is important to note that the quenching experiment was done in-well and did not undergo the same steps as homogenates. Mainly, when homogenates have been treated with their respective reagents, they undergo a desalting step in order to remove excess $\text{H}_2\text{O}_2+\text{NaI}$ and TCEP, while in the quenching experiment dye was added directly to solutions containing their respective reagents. Thus, while the quenching data suggests a decrease in fluorescence in the presence of the reagents, we would expect even less of an interaction after desalting as is done with homogenates. However, we have not yet eliminated the possibility that residual reagents may be left over after desalting which could be interfering at some level with our dye.

6C - Effects of Reducing and Oxidizing samples on IRDye800CW Maleimide fluorescence

Our first method for manipulating the redox state of our lysates involved the use of $\text{H}_2\text{O}_2+\text{NaI}$ as our oxidizing agent and TCEP as our reducing agent. As seen in Figure 7, the oxidized group had a much lower signal than control. For our reduced group we expected to find a greater signal than control. Interestingly, however, our reduced condition in gel also significantly lowered fluorescence when normalized to control while absolute values showed a

trending, albeit non-significant decrease. While this finding may partly be due to dye quenching caused by residual TCEP left after desalting, we questioned whether TCEP was an effective reducing agent. At the same time, we wondered whether the physiological state of most proteomic cysteines exist in the reduced state, thereby preventing our signal to increase above control levels. In order to guide our understanding towards these questions we needed to develop a way to test the efficacy of TCEP as a reducing agent.

6D - TCEP returns fluorescence of Oxidized samples to Control Levels

By incorporating a ‘rescue’ condition in which we subsequently oxidized and reduced the sample, we would be able to better determine the reducing power of TCEP. Our in-gel data shows that following oxidation, TCEP was able to return fluorescence back to control levels (Figure 8a) even while the reduced condition continued to show a drop in signal when normalized to control (Figure 8b, inset) although no significant decrease was found when considering absolute fluorescence (Figure 8b). Our plate data shows similar results with the oxidized and rescue groups (Figure 9a) but what is important to note with this set of data is that the reduced condition shows a significant increase in signal compared to control (Figure 9b) while the in-gel data shows a trending decrease after reduction (Figure 8b). Similarly, the rescue condition in plate also trends towards an increase in signal while the in-gel rescue condition is slightly lower than control. We have not yet determined the exact cause of this discrepancy between gel and plate in the TCEP treated samples. One possible cause is that the in-gel method separates proteins based on molecular weight and has an upper limit of 250kDa based on western protocol. Furthermore, our in-gel analysis covers the range of 25-100kDa. While this allows us to discriminate between proteins and their redox states within that range, it removes information

beyond these upper and lower limits. It is possible that the plate data incorporates more redox sensitive proteins (even with the same amount of total protein as the gels) leading to a greater signal compared to the in-gel fluorescence.

What is interesting to notice as well with our TCEP experiments is that not all bands showed greater fluorescence compared to control. The fluorescence of the 37kDa band, for example, decreases in TCEP-treated samples compared to control. It is not yet clear why this occurs however it may suggest that not all proteins share the same ability to be reduced. It is possible that certain proteins that exist in a reduced state are close to the reductive limit of the protein such that any further reduction will lead to 'reductive stress'. Indeed, it has been shown that cardiac mitochondria increase the rate of ROS production in states of reductive stress⁸⁶ and certain proteins may therefore be more susceptible to oxidation by ROS produced in this fashion.

In order to confirm the validity of our findings using the IRDye800CW Maleimide using both the in-gel and plate approach, we determined the level of GSH, GSSG and the ratio of GSH/GSSG (Figure 10). Control and reduced groups all showed similar GSH content (Figure 10, a2) with similar findings in GSSG content (Figure 10, b2) and the GSH:GSSG ratio (Figure 10, c2). The increase in GSSG content for the oxidized group suggests a higher level of oxidation occurred with this treatment while the other conditions showed no difference in GSSG content (Figure 10, b1). All conditions showed no differences in GSH content (Figure 10, a1) and the GSH:GSSG ratio (Figure 10, c1). The observations made with GSSG content in these samples present a case where the dye could be more predictive of GSSG content rather than GSH content. They also indicate that the IRDye800CW Maleimide closely follows the GSSG and GSH/GSSG ratio patterns measured with HPLC suggesting that it may be used as a strong predictor of cellular redox state.

6E - 49⁰C heat treatment lowers IRDye800CW Maleimide fluorescence

To follow up with our chemically-induced changes to redox state of lysates, we moved forward by manipulating redox states using heat since this is known to increase markers of oxidative stress such as thiobarbituric acid reactive substances (TBARS)⁸⁴ and DNA degradation⁸⁷. It has previously been shown that 42⁰C temperatures in rat tissue showed a time-dependent increase in ROS production⁸⁸. Furthermore, rats with core temperatures of 42⁰C showed an increase in markers of oxidative stress which subsided after a given amount of recovery time⁸⁷. Given these findings, we were interested using heat as one of our models for altering cellular redox states and we chose 49⁰C to ensure sufficient oxidation in cells, potentially leading to irreversible oxidative modifications such as carbonylation. As expected, we saw a significant decrease in fluorescence after heat-exposure, suggesting that proteins have been oxidized and that the dye was accurately able to capture these differences in-gel at the 25-100kDa range using our direct method (Figure 11e) and using the in-well approach (Figure 12).

While we noticed a drop in overall fluorescence after heating, specific bands of the proteome were also assessed to determine their influence on the overall 25-100kDa fluorescence. Our attention shifted to the bands located at 25kDa (Figure 11b), 44kDa (Figure 11c) and 60kDa (Figure 11d) since these regions showed a trending increase in fluorescence after 49⁰C heat treatment. The reasons for these observations have yet to be determined however we speculate that spatial separation and localization of specific redox sensitive proteins may play a role. Indeed, it has been found that different cysteine residues are localized such that they possess a range of pKa values leading to a range of reactivity with oxidizing and reducing environments². This notion of compartmentalization also provides a means of specificity for cysteines to react with ROS/RNS since there is no direct receptor for the molecules.

We were interested in comparing our method to a previously published approach used by Requejo et al.⁷⁹ in which samples were first treated with N-ethylmaleimide (NEM) to irreversibly block all reduced thiols. This leaves all reversibly oxidized proteins untouched until a reducing compound is added (such as TCEP). The newly reduced thiols are then labeled with a maleimide-based dye similar to IRDye800CW and the measured fluorescence densitometry represents proteins that were initially in the oxidized state. It has been suggested that this ‘difference in gel electrophoresis’ (DIGE) method of indirectly measuring oxidized proteins is more sensitive than measuring reduced thiols⁷⁹. However, a limitation to this DIGE method is that it can only provide information on reversible thiol modifications whereas the present method would in theory reflect all forms of oxidation. While this may be an important consideration for particular research questions, it does not allow researchers to investigate questions regarding total redox states. In order to confirm which method would provide more sensitivity with respect to proteomic redox states we compared our direct method with the DIGE method for our heat experiments. In doing so, we expected to see a drop in signal after heating using the direct method, while the DIGE method would show the opposite with heat treatment increasing fluorescence. As seen from the results in panel e of Figure 11, the DIGE method did not work in our hands since fluorescence of the 25-100kDa range dropped after oxidation with 49⁰C. We suspected that this may be caused by irreversible oxidation caused by the high temperature. To test this possibility, we proceeded to compare the two methods using 40⁰C heat (discussed below) which is considered to be high enough to cause oxidation but low enough to it reversible⁸⁷.

As a tool for validating IRDye800CW Maleimide we again measured GSH and GSSG content to see if a relationship existed between fluorescence and cellular redox state after 49⁰C incubations. While this heat treatment did not change GSH content (Figure 13a), GSSG content

showed a significant increase (Figure 13b) with a concomitant decrease in the GSH/GSSG ratio (Figure 13c). This increase in GSSG may be attributed to an increase in glutathionylated proteins as a result of high heat which is known to create an oxidative environment⁸⁹. Nevertheless, this data suggests that the dye may be used to determine GSSG content in homogenates.

6F - 40°C heat treatment has no significant effect on IRDye800CW Maleimide fluorescence

By lowering the temperature of our oxidized group to 40°C, we expected to find smaller differences between control and heated samples using our direct method since this temperature leads to less oxidative stress compared to 49°C⁸⁷. Indeed, our 25-100kDa in-gel (Figure 14e) and the plate assay (Figure 15) showed no significant difference between control and heated samples suggesting that oxidation was minimal and that IRDye800CW Maleimide fluorescence corresponds to the level of reduced proteins. In line with our 49°C results, the three specified bands at 25, 44 and 60kDa showed a trending increase in fluorescence after heating. As discussed above, one possibility for this might be spatially-determined specificity and compartmentalization.

We dropped the temperature of our heated group to 40°C in-part to determine whether our failed attempts at the DIGE method had to do with irreversible oxidation caused by 49°C heat. Figure 14 DIGE results show that this issue was not resolved with this change since the oxidized samples continued to show decreased fluorescence compared to control as we expect to see the opposite with this method. It is still unclear why the DIGE method has failed in our hands however one consideration is the dyes used for the experiments. We have optimized our direct protocol for use with the IRDye800CW Maleimide and have validated this dye through a number

of methods presented in this paper however Requejo et al. used a Cy3 and Cy5 fluorophores in their DIGE methods⁷⁹.

GSH content (Figure 16a) and GSH/GSSG ratios (Figure 16c) showed a significant drop after 40⁰C treatment while GSSG content showed a trending yet insignificant increase (Figure 16b). Once again this closely follows the data observed with direct in-gel whole-lane fluorescence (Figure 14e) and plate fluorescence (Figure 15) for the 40⁰C treatment presenting yet another case where IRDye800CW Maleimide fluorescence is related to GSSG content.

6G - 49⁰C heat significantly increases protein carbonylation while 40⁰C does not

In order to address whether our selected temperatures were causing reversible or irreversible oxidation, we included an experiment to look at carbonylation of proteins since this is a form of irreversible protein oxidation. As expected we found that there was a significant increase in carbonylated proteins with 49⁰C (Figure 17b) while 40⁰C heat led to no change relative to control (Figure 17a). IRDye800CW Maleimide fluorescence is very closely related to protein carbonylation such that wherever a significant increase in carbonyl products occurs (49⁰C, Figure 17b) there is a significant decrease in dye fluorescence in-gel (Figure 11e) and in plate (Figure 12). The same relationship holds true in the 40⁰C group where no significance was observed in carbonylation (Figure 17a), in-gel fluorescence (Figure 14e) and in plate (Figure 15).

Chapter 7: Conclusions and Future Directions

7A - Conclusions

This study was aimed at validating the IRDye800CW Maleimide as a useful tool for accurately detecting the redox state of lysates. While there are currently highly sensitive methods available, such as mass spectrometry and HPLC, access to these instruments may be limited to some researchers due to their high cost and technical expertise. Given these accessibility barriers, these labs may not have the resources or the training required to use these instruments but instead possess laboratory infrastructure for western blotting or microplate assays. As such, it is important for researchers to have an affordable and reliable option to directly detect protein redox states using a method that can be incorporated into commonly used assays such as SDS-PAGE and in-well assays. Here, we have taken multiple approaches to test whether the changes observed in the dye's fluorescence match results of redox state measured through GSH and GSSG content as well as protein carbonylation. We can conclude, based on the evidence presented in this study, that the IRDye800CW Maleimide does accurately represent the redox state in homogenates. Our target audience is the researchers who are interested in analyzing redox states of samples but whose primary focus is not redox bioenergetics. This method offers a simplified and affordable approach for such labs to accurately detect the redox state of proteins in samples. While the IRDye800CW Maleimide does not provide information regarding the specific form of oxidative modification that has occurred, this limitation presents one of its greatest strengths in that it accurately captures all forms of oxidation and reduction in a given sample providing researchers with a wealth of information related to redox states.

7B – Future Directions

The data we have presented thus far all involves a form of in vitro modification of redox states, whether through treating homogenates with different reagents or via exposure to heat. Since many researchers are interested in looking at in-vivo models, we would be interested in testing IRDye800CW Maleimide under such conditions that can bring about change in cellular redox states. One potential avenue of doing this is by looking at tissue that has gone through an acute bout of exercise or dietary influences since these are known to increase oxidation⁹⁸. Certain disease conditions, such as muscular dystrophy, Alzheimer's and Parkinson's, have also shown to have elevated levels of ROS and oxidative stress⁹⁹⁻¹⁰¹.

We have demonstrated that desalting homogenates prior to labeling with the dye greatly enhances our signal. While we show that endogenous glutathione plays a role in this finding, it does not appear to be the only factor. It would be useful to determine the levels of other thiol-containing compounds, such as free cysteines and coenzyme A, after desalting. Furthermore, it would be useful to determine whether or not the desalting columns are completely removing our reagents since we have shown that there is a quenching effect between the dye and the reagents. The hypothesis that not all reagents are being removed by desalting would be consistent with our findings in Figure 8 where our TCEP-treated samples show lower fluorescence than control. If this is the case then our current findings with IRDye800CW Maleimide in both oxidized and reduced samples could be an underestimation of what is really occurring. Therefore it is important for us to determine the levels of H_2O_2+NaI and TCEP after desalting.

Finally, to compare the sensitivities of the direct detection of thiols versus the indirect DIGE method, we must resolve our results with the DIGE method. A potential avenue to consider is the use of dyes. Our direct method incorporates the IRDye800CW Maleimide and this is the dye we used when attempting the DIGE method. However Requejo et al used the Cy3 and

Cy5. Although all of these dyes have similar properties (i.e. being maleimides) they may still contain differences that require consideration when used in homogenates. Future studies comparing these two methods may need to consider these differences.

References

1. Cadenas, E. & Davies, K. J. Mitochondrial free radical generation, oxidative stress, and aging. *Free Radic. Biol. Med.* **29**, 222–230 (2000).
2. Jones, D. P. Radical-free biology of oxidative stress. (2008). doi:10.1152/ajpcell.00283.2008.
3. Jenner, P. Oxidative stress in Parkinson's disease. *Ann. Neurol.* **53 Suppl 3**, S26–36; discussion S36–8 (2003).
4. Gracy, R. W., Talent, J. M., Kong, Y. & Conrad, C. C. Reactive oxygen species: The unavoidable environmental insult? *Mutat. Res. - Fundam. Mol. Mech. Mutagen.* **428**, 17–22 (1999).
5. Ragusa, R. J., Chow, C. K. & Porter, J. D. Oxidative stress as a potential pathogenic mechanism in an animal model of Duchenne muscular dystrophy. *Neuromuscul. Disord.* **7**, 379–86 (1997).
6. Ray, P. D., Huang, B.-W. & Tsuji, Y. Reactive oxygen species (ROS) homeostasis and redox regulation in cellular signaling. *Cell. Signal.* **24**, 981–90 (2012).
7. Finkel, T. Signal transduction by reactive oxygen species. *J. Cell Biol.* **194**, 7–15 (2011).
8. Go, Y.-M. & Jones, D. P. The Redox Proteome. *J. Biol. Chem.* **288**, 26512–26520 (2013).
9. Davies, M. J. Free radicals, oxidants and protein damage. *Aust. Biochem.* **43**, 8–12 (2012).
10. Jackson, M. J. Redox regulation of adaptive responses in skeletal muscle to contractile activity. *Free Radic. Biol. Med.* **47**, 1267–75 (2009).
11. Schieber, M. & Chandel, N. S. ROS function in redox signaling and oxidative stress. *Curr. Biol.* **24**, R453–R462 (2014).
12. Ushio-Fukai, M. Compartmentalization of redox signaling through NADPH oxidase-derived ROS. *Antioxid. Redox Signal.* **11**, 1289–1299 (2009).

13. Frazziano, G. *et al.* Nox-derived ROS are acutely activated in pressure overload pulmonary hypertension: indications for a seminal role for mitochondrial Nox4. *Am. J. Physiol. Heart Circ. Physiol.* **306**, H197–205 (2014).
14. Bedard, K. & Krause, K.-H. The NOX family of ROS-generating NADPH oxidases: physiology and pathophysiology. *Physiol. Rev.* **87**, 245–313 (2007).
15. Kelley, E. E. *et al.* Hydrogen peroxide is the major oxidant product of xanthine oxidase. *Free Radic. Biol. Med.* **48**, 493–498 (2010).
16. Kong, L. D., Cai, Y., Huang, W. W., Cheng, C. H. K. & Tan, R. X. Inhibition of xanthine oxidase by some Chinese medicinal plants used to treat gout. *J. Ethnopharmacol.* **73**, 199–207 (2000).
17. Harrison, R. Physiological roles of xanthine oxidoreductase. *Drug Metab. Rev.* **36**, 363–75 (2004).
18. Montezano, A. C. & Touyz, R. M. Reactive oxygen species and endothelial function--role of nitric oxide synthase uncoupling and Nox family nicotinamide adenine dinucleotide phosphate oxidases. *Basic Clin. Pharmacol. Toxicol.* **110**, 87–94 (2012).
19. Scatena, R., Bottoni, P. & Giardina, B. *Advances in Mitochondrial Medicine. Advances in Experimental Medicine and Biology* **942**, (2012).
20. Gupta, R. K. *et al.* Oxidative stress and antioxidants in disease and cancer: a review. *Asian Pac. J. Cancer Prev.* **15**, 4405–9 (2014).
21. Bates, J. T. *et al.* Reactive Oxygen Species Generation Linked to Sources of Atmospheric Particulate Matter and Cardiorespiratory Effects. *Environ. Sci. Technol.* acs.est.5b02967 (2015). doi:10.1021/acs.est.5b02967
22. Hurd, T. R. *et al.* Inactivation of pyruvate dehydrogenase kinase 2 by mitochondrial reactive oxygen species. *J. Biol. Chem.* **287**, 35153–60 (2012).
23. Mailloux, R. J., Jin, X. & Willmore, W. G. Redox regulation of mitochondrial function with emphasis on cysteine oxidation reactions. *Redox Biol.* **2**, 123–139 (2014).
24. Storz, P. Reactive oxygen species in tumor progression. *Front Biosci* **10**, 1881–1896 (2005).

25. Valko, M., Rhodes, C. J., Moncol, J., Izakovic, M. & Mazur, M. Free radicals, metals and antioxidants in oxidative stress-induced cancer. *Chem. Biol. Interact.* **160**, 1–40 (2006).
26. Hill, B. G., Reily, C., Oh, J.-Y., Johnson, M. S. & Landar, A. Methods for the determination and quantification of the reactive thiol proteome. *Free Radic. Biol. Med.* **47**, 675–83 (2009).
27. Finkel, T. From Sulfenylation to Sulfhydration: What a Thiolate Needs to Tolerate. *Sci. Signal.* **5**, pe10–pe10 (2012).
28. Brandes, N., Schmitt, S. & Jakob, U. Thiol-based redox switches in eukaryotic proteins. *Antioxid. Redox Signal.* **11**, 997–1014 (2009).
29. Leonard, S. E., Reddie, K. G. & Carroll, K. S. Mining the thiol proteome for sulfenic acid modifications reveals new targets for oxidation in cells. *ACS Chem. Biol.* **4**, 783–799 (2009).
30. Leichert, L. I. *et al.* Quantifying changes in the thiol redox proteome upon oxidative stress in vivo. *Proc. Natl. Acad. Sci. U. S. A.* **105**, 8197–8202 (2008).
31. Wang, H. *et al.* Proteomic analysis of early-responsive redox-sensitive proteins in Arabidopsis. *J. Proteome Res.* **11**, 412–24 (2012).
32. The_disulfide_proteome_and_oth.PDF.
33. Hurd, T. R., Prime, T. A., Harbour, M. E., Lilley, K. S. & Murphy, M. P. Detection of Reactive Oxygen Species-sensitive Thiol Proteins by Redox Difference Gel Electrophoresis: IMPLICATIONS FOR MITOCHONDRIAL REDOX SIGNALING. *J. Biol. Chem.* **282**, 22040–22051 (2007).
34. den Hertog, J., Groen, A. & van der Wijk, T. Redox regulation of protein-tyrosine phosphatases. *Arch Biochem Biophys* **434**, 11–15 (2005).
35. Mohr, S., Hallak, H., De Boitte, A., Lapetina, E. G. & Brüne, B. Nitric oxide-induced S-glutathionylation and inactivation of glyceraldehyde-3-phosphate dehydrogenase. *J. Biol. Chem.* **274**, 9427–9430 (1999).

36. Ng, C. F., Schafer, F. Q., Buettner, G. R. & Rodgers, V. G. J. The rate of cellular hydrogen peroxide removal shows dependency on GSH: mathematical insight into in vivo H₂O₂ and GPx concentrations. *Free Radic. Res.* **41**, 1201–11 (2007).
37. Ng, C. F., Schafer, F. Q., Buettner, G. R. & Rodgers, V. G. The rate of cellular hydrogen peroxide removal shows dependency on GSH: mathematical insight into in vivo H₂O₂ and GPx concentrations. *Free Radic Res* **41**, 1201–1211 (2007).
38. Anderson, E. J. *et al.* Mitochondrial H₂O₂ emission and cellular redox state link excess fat intake to insulin resistance in both rodents and humans. *J Clin Invest* **119**, 573–581 (2009).
39. Stadtman, E. R. Serial Review : Oxidative Stress and Aging. *Free Radic. Biol. Med.* **33**, 597– 604 (2002).
40. Junqueira, V. B. C. *et al.* Aging and oxidative stress. *Mol. Aspects Med.* **25**, 5–16 (2004).
41. Terrill, J. R. *et al.* Oxidative stress and pathology in muscular dystrophies: Focus on protein thiol oxidation and dysferlinopathies. *FEBS J.* **280**, 4149–4164 (2013).
42. Shkryl, V. M. *et al.* Reciprocal amplification of ROS and Ca²⁺ signals in stressed mdx dystrophic skeletal muscle fibers. *Pflugers Arch. Eur. J. Physiol.* **458**, 915–928 (2009).
43. Renjini, R., Gayathri, N., Nalini, a. & Bharath, M. M. S. Oxidative damage in muscular dystrophy correlates with the severity of the pathology: Role of glutathione metabolism. *Neurochem. Res.* **37**, 885–898 (2012).
44. Tidball, J. G. & Wehling-Henricks, M. The role of free radicals in the pathophysiology of muscular dystrophy. *J. Appl. Physiol.* **102**, 1677–1686 (2006).
45. Anderson, E. J. *et al.* Substrate-specific derangements in mitochondrial metabolism and redox balance in the atrium of the type 2 diabetic human heart. *J. Am. Coll. Cardiol.* **54**, 1891–8 (2009).
46. Martín-Gallán, P., Carrascosa, A., Gussinyé, M. & Domínguez, C. Biomarkers of diabetes-associated oxidative stress and antioxidant status in young diabetic patients with or without subclinical complications. *Free Radic. Biol. Med.* **34**, 1563–1574 (2003).
47. Furukawa, S. *et al.* Increased oxidative stress in obesity and its impact on metabolic syndrome. *J. Clin. Invest.* **114**, 1752–1761 (2004).

48. Keaney, J. F. *et al.* Obesity and systemic oxidative stress: Clinical correlates of oxidative stress in the Framingham study. *Arterioscler. Thromb. Vasc. Biol.* **23**, 434–439 (2003).
49. Shahnawaz Khan, M., Tabrez, S., Priyadarshini, M., Priyamvada, S. & Khan, M. M. Targeting Parkinsons-Tyrosine Hydroxylase and Oxidative Stress as Points of Interventions. *CNS Neurol. Disord. - Drug Targets* **11**, 369–380 (2012).
50. Noda, N. & Wakasugi, H. Cancer and Oxidative Stress. *Jmaj* **44**, 535–539 (2001).
51. Brown, N. S. & Bicknell, R. Hypoxia and oxidative stress in breast cancer. Oxidative stress: its effects on the growth, metastatic potential and response to therapy of breast cancer. *Breast Cancer Res.* **3**, 323–327 (2001).
52. Toyokuni, S., Okamoto, K., Yodoi, J. & Hiai, H. Persistent oxidative stress in cancer. *FEBS Lett.* **358**, 1–3 (1995).
53. Yoritaka, a *et al.* Immunohistochemical detection of 4-hydroxynonenal protein adducts in Parkinson disease. *Proc. Natl. Acad. Sci. U. S. A.* **93**, 2696–2701 (1996).
54. Floor, E. & Wetzel, M. G. Increased protein oxidation in human substantia nigra pars compacta in comparison with basal ganglia and prefrontal cortex measured with an improved dinitrophenylhydrazine assay. *J. Neurochem.* **70**, 268–75 (1998).
55. Alam, Z. I. *et al.* Oxidative DNA damage in the parkinsonian brain: an apparent selective increase in 8-hydroxyguanine levels in substantia nigra. *J. Neurochem.* **69**, 1196–1203 (1997).
56. Zhang, J. *et al.* Parkinson's disease is associated with oxidative damage to cytoplasmic DNA and RNA in substantia nigra neurons. *Am. J. Pathol.* **154**, 1423–9 (1999).
57. Good, P. F., Werner, P., Hsu, a, Olanow, C. W. & Perl, D. P. Evidence of neuronal oxidative damage in Alzheimer's disease. *Am. J. Pathol.* **149**, 21–28 (1996).
58. Hensley, K. *et al.* Brain regional correspondence between Alzheimer's disease histopathology and biomarkers of protein oxidation. *J. Neurochem.* **65**, 2146–2156 (1995).
59. Miranda, M. D., de Bruin, V. M. S., Vale, M. R. & Viana, G. S. B. Lipid peroxidation and

nitrite plus nitrate levels in brain tissue from patients with Alzheimer's disease. *Gerontology* **46**, 179–184 (2000).

60. Marcus, D. L. *et al.* Increased peroxidation and reduced antioxidant enzyme activity in Alzheimer's disease. *Exp. Neurol.* **150**, 40–44 (1998).
61. Palmer, A. M. & Burns, M. A. Selective increase in lipid peroxidation in the inferior temporal cortex in Alzheimer's disease. *Brain Res.* **645**, 338–342 (1994).
62. Smith, C. D. *et al.* Excess brain protein oxidation and enzyme dysfunction in normal aging and in Alzheimer disease. *Proc. Natl. Acad. Sci. U. S. A.* **88**, 10540–3 (1991).
63. Kumar, A., Singh, A. & Ekavali. A review on Alzheimer's disease pathophysiology and its management: an update. *Pharmacol. Rep.* **67**, 195–203 (2015).
64. Markesbery, W. R. & Lovell, M. A. Four-hydroxynonenal, a product of lipid peroxidation, is increased in the brain in Alzheimer's disease. *Neurobiol. Aging* **19**, 33–36 (1998).
65. Emwas, A.-H. M. The strengths and weaknesses of NMR spectroscopy and mass spectrometry with particular focus on metabolomics research. *Methods Mol. Biol.* **1277**, 161–93 (2015).
66. Amstalden van Hove, E. R., Smith, D. F. & Heeren, R. M. a. A concise review of mass spectrometry imaging. *J. Chromatogr. A* **1217**, 3946–3954 (2010).
67. Butterfield, D. A., Gu, L., Domenico, F. Di & Robinson, R. a S. Mass spectrometry and redox proteomics: Applications in disease. *Mass Spectrom. Rev.* **33**, 277–301 (2014).
68. Huang, Y. *et al.* Mass spectrometry-based metabolomic profiling identifies alterations in salivary redox status and fatty acid metabolism in response to inflammation and oxidative stress in periodontal disease. *Free Radic. Biol. Med.* **70**, 223–232 (2014).
69. Pan, K.-T. *et al.* Mass Spectrometry-Based Quantitative Proteomics for Dissecting Multiplexed Redox Cysteine Modifications in Nitric Oxide-Protected Cardiomyocyte Under Hypoxia. *Antioxid. Redox Signal.* **20**, 1365–1381 (2014).
70. Schafer, F. Q. & Buettner, G. R. Redox environment of the cell as viewed through the redox state of the glutathione disulfide/glutathione couple. *Free Radic. Biol. Med.* **30**, 1191–212 (2001).

71. Han, D., Canali, R., Rettori, D. & Kaplowitz, N. Effect of glutathione depletion on sites and topology of superoxide and hydrogen peroxide production in mitochondria. *Mol. Pharmacol.* **64**, 1136–44 (2003).
72. Sloan, R. C. *et al.* Mitochondrial permeability transition in the diabetic heart: contributions of thiol redox state and mitochondrial calcium to augmented reperfusion injury. *J. Mol. Cell. Cardiol.* **52**, 1009–18 (2012).
73. Foster, M. W., Hess, D. T. & Stamler, J. S. Protein S-nitrosylation in health and disease: a current perspective. *Trends Mol. Med.* **15**, 391–404 (2009).
74. Gupta, V. & Carroll, K. S. Sulfenic acid chemistry, detection and cellular lifetime. *Biochim. Biophys. Acta - Gen. Subj.* **1840**, 847–875 (2014).
75. Wang, P. & Powell, S. R. Decreased sensitivity associated with an altered formulation of a commercially available kit for detection of protein carbonyls. *Free Radical Biology and Medicine* **49**, 119–121 (2010).
76. Tyagarajan, K., Pretzer, E. & Wiktorowicz, J. E. Thiol-reactive dyes for fluorescence labeling of proteomic samples. *Electrophoresis* **24**, 2348–2358 (2003).
77. Eaton, P. Protein thiol oxidation in health and disease: techniques for measuring disulfides and related modifications in complex protein mixtures. *Free Radic. Biol. Med.* **40**, 1889–99 (2006).
78. Wall, S. B. *et al.* Detection of electrophile-sensitive proteins. *Biochim. Biophys. Acta - Gen. Subj.* **1840**, 913–922 (2014).
79. Requejo, R. *et al.* Quantification and identification of mitochondrial proteins containing vicinal dithiols. *Arch. Biochem. Biophys.* **504**, 228–35 (2010).
80. Riederer, I. M., Herrero, R. M., Leuba, G. & Riederer, B. M. Serial protein labeling with infrared maleimide dyes to identify cysteine modifications. *J. Proteomics* **71**, 222–30 (2008).
81. Tyagarajan, K., Pretzer, E. & Wiktorowicz, J. E. Thiol-reactive dyes for fluorescence labeling of proteomic samples. *Electrophoresis* **24**, 2348–2358 (2003).

82. van der Poel, C. & Stephenson, D. G. Effects of elevated physiological temperatures on sarcoplasmic reticulum function in mechanically skinned muscle fibers of the rat. *Am. J. Physiol. Cell Physiol.* **293**, C133–C141 (2007).
83. van der Poel, C. & Stephenson, D. G. Reversible changes in Ca²⁺-activation properties of rat skeletal muscle exposed to elevated physiological temperatures. *J. Physiol.* **544**, 765–776 (2002).
84. Lin, H., Decuypere, E. & Buyse, J. Acute heat stress induces oxidative stress in broiler chickens. *Comp. Biochem. Physiol. A. Mol. Integr. Physiol.* **144**, 11–17 (2006).
85. Lushchak, V. I. Glutathione Homeostasis and Functions: Potential Targets for Medical Interventions. *J. Amino Acids* **2012**, 1–26 (2012).
86. Korge, P., Calmettes, G. & Weiss, J. N. Increased reactive oxygen species production during reductive stress: The roles of mitochondrial glutathione and thioredoxin reductases. *Biochim. Biophys. Acta - Bioenerg.* **1847**, 514–525 (2015).
87. Ippolito, D. L., Lewis, J. A., Yu, C., Leon, L. R. & Stallings, J. D. Alteration in circulating metabolites during and after heat stress in the conscious rat : potential biomarkers of exposure and organ-specific injury. *Bmc Physiol.* **14**, 1–17 (2014).
88. Zuo, L. *et al.* Intra- and extracellular measurement of reactive oxygen species produced during heat stress in diaphragm muscle. *Am. J. Physiol. Cell Physiol.* **279**, C1058–C1066 (2000).
89. Belhadj Slimen, I. *et al.* Reactive oxygen species, heat stress and oxidative-induced mitochondrial damage. A review. *Int. J. Hyperth.* **30**, 513–523 (2014).
90. Frasier, C. R. *et al.* Redox-dependent increases in glutathione reductase and exercise preconditioning: Role of NADPH oxidase and mitochondria. *Cardiovasc. Res.* **98**, 47–55 (2013).
91. Sloan, R. C. *et al.* Mitochondrial permeability transition in the diabetic heart: Contributions of thiol redox state and mitochondrial calcium to augmented reperfusion injury. *J. Mol. Cell. Cardiol.* **52**, 1009–1018 (2012).
92. bio SYNTHESIS. Instruction of reduction reaction using TCEP. at <<http://www.biosyn.com/tew/instruction-of-reduction-reaction-using-tcep.aspx>>

93. Madanská, J., Vitková, Z. & Capková, Z. [Examination of the stability of hydrogen peroxide solutions]. *Ces. a Slov. Farm. Cas. Ces. Farm. Spol. a Slov. Farm. Spol.* **53**, 261–3 (2004).
94. Lukesh, J. C., Palte, M. J. & Raines, R. T. A potent, versatile disulfide-reducing agent from aspartic acid. *J. Am. Chem. Soc.* **134**, 4057–4059 (2012).
95. Shafer, D. E., Inman, J. K. & Lees, A. Reaction of Tris(2-carboxyethyl)phosphine (TCEP) with maleimide and alpha-haloacyl groups: anomalous elution of TCEP by gel filtration. *Anal. Biochem.* **282**, 161–164 (2000).
96. Luo, D., Smith, S. W. & Anderson, B. D. Kinetics and mechanism of the reaction of cysteine and hydrogen peroxide in aqueous solution. *J. Pharm. Sci.* **94**, 304–316 (2005).
97. Mitić, S. S., Miletić, G. Z. & Kostić, D. a. Kinetic determination of traces of iodide by its catalytic effect on oxidation of sodium pyrogallol-5-sulfonate by hydrogen peroxide. *Anal. Sci.* **19**, 913–6 (2003).
98. Sastre, J. & Asensi, M. Exhaustive physical exercise causes oxidation of glutathione status in blood: prevention by antioxidant administration. *Am. J. Physiol. Regul. Integr. Comp. Physiol.* **263**, R992–R995 (1992).
99. Shin, J., Tajrishi, M. M., Ogura, Y. & Kumar, A. Wasting mechanisms in muscular dystrophy. *Int. J. Biochem. Cell Biol.* **45**, 2266–2279 (2013).
100. Yana, M. H., Wang, X. & Zhu, X. Mitochondrial defects and oxidative stress in Alzheimer disease and Parkinson disease. *Free Radical Biology and Medicine* **62**, 90–101 (2013).
101. Dias, V., Junn, E. & Mouradian, M. M. The role of oxidative stress in parkinson's disease. *Journal of Parkinson's Disease* **3**, 461–491 (2013).

Appendix A – Optimization Process for IRDye800CW Maleimide

Prior to beginning our experiments with IRDye800CW Maleimide, we intended to mimic the protocol presented by Sloan et al. in which they used PBS (pH 7.5) with 5mM DTT as their reducing agent and 5mM H₂O₂ as their oxidizing agent^{72,90}. We did this in order to determine whether we would obtain similar results before proceeding with other forms of validation. In our attempts at this method, we were unable to repeat the findings obtained from these two studies. As previously shown in our results, one of the key steps that had to be incorporated to our assay was desalting samples prior to dye labeling (Figure 4 and 5). Once this first problem was addressed, we were able to continue our troubleshooting process.

A1. Assay Buffer

Following previous protocols^{90,91} our initial redox assays were done in PBS, however as described below in our optimizing procedures, we switched from DTT to TCEP as our reducing agent, which required a buffer change as well since TCEP is considered to be less stable in phosphate buffers at neutral pH⁹². We attempted the assay in both CHAPS and Tris buffers due to their low cost and ease of preparation and we found that both buffers yielded similar results, although fluorescence seemed to be greater and more consistent in Tris for all conditions compared to CHAPS (data not shown).

A2. Incubation Conditions

As seen in Supplemental Figure 1 in Appendix B, we obtained results that were opposite from what we expected such that the DTT samples were less fluorescent than control and H₂O₂ samples were more fluorescent than control. We speculated that the reasons why DTT and H₂O₂-

treated samples did not match previously reported findings might have to do with our incubation parameters. We had started by incubating samples for 1 hour on a rocker at room temperature however this did not resolve our issues (data not shown). We speculated that the reaction between thiols and our reagents was not occurring fast enough therefore we decided to incubate for 1 hour at 37°C in an attempt to speed up the reaction of thiol groups with DTT and H₂O₂ but this did not improve our signal. Once we decreased the incubation period to 30 minutes at room temperature we began to notice improvements in our H₂O₂-treated samples which showed less fluorescence than previous experiments. In accordance with these findings, it has been suggested that hydrogen peroxide is an unstable compound that is both temperature and light sensitive⁹³. Given our findings with incubation time and temperature, it may be possible that 1 hour exposure of H₂O₂ to room temperature or higher is enough to degrade the compound and prevent effective oxidation of thiols in homogenate. Although these incubation parameters improved our H₂O₂ signals compared to previous experiments, results using these incubation times still showed greater fluorescence with H₂O₂ relative to controls (data not shown). Therefore, we looked to other solutions for troubleshooting our protocol before determining our ideal incubation parameters.

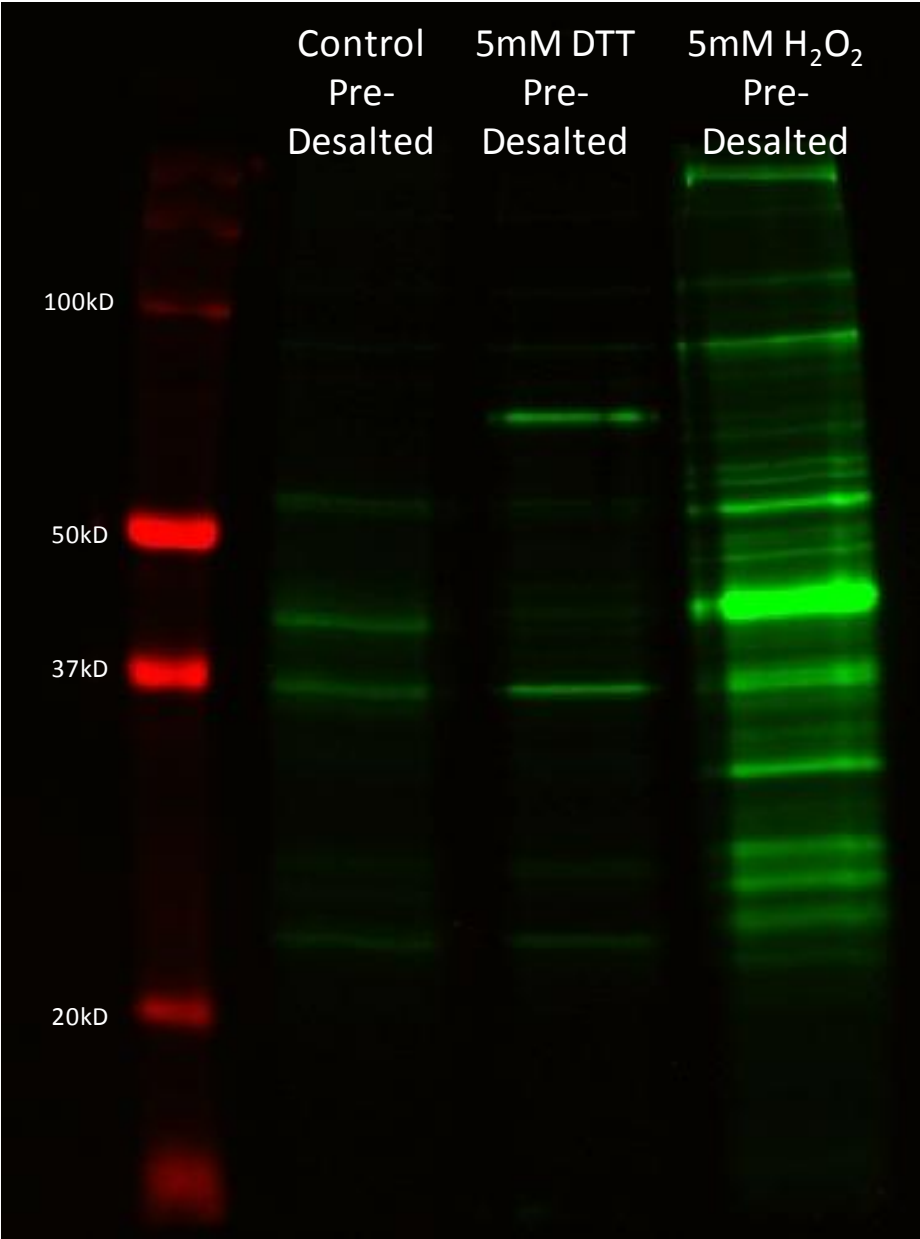
A3. DTT and H₂O₂

In order to address our low DTT signal and high H₂O₂ signal we questioned whether these compounds were effective enough to cause changes in thiol groups in homogenates. DTT is a commonly used reducing agent but it has been suggested that DTT may actually be a poor reducing agent due to its low reactivity at neutral pH⁹⁴ which is near the effective pH range of the IRdye800CW-Maleimide (6.5-7.5). Because of its pK_a value, the thiolate anions of DTT are

protonated and therefore unreactive at neutral pH, with only 1% of its thiols reportedly being reactive⁹⁴. Consistent with this finding, our initial results with DTT demonstrate that at a pH of 7.5, DTT incubations were not effective at increasing fluorescent intensity as compared to untreated samples (Supplemental Figure 1, Appendix B). Given the reports and our findings on DTT, we began implementing tris (2-carboxyethyl) phosphine (TCEP) as a reducing agent. TCEP is another commonly used reducing agent which has been reported to show stability across a wide pH of 1.5-8.5^{95,96}. After incorporating TCEP into our samples we found IRDye800CW-Maleimide's absolute fluorescence values showed no difference while normalized values showed a significant decrease in fluorescence (Figure 7). Given our observations with the effective rescue condition of TCEP (Figure 8), we proceeded with this reducing agent for the remainder of our optimization.

We suspected that H₂O₂ was not working because it lacked sufficient stability to react with thiols in the 30 minutes we allowed it to incubate in our samples. As such, we decided to add sodium iodide to our H₂O₂ solution since this is known to be a catalyst in the reaction between H₂O₂ and thiols⁹⁷. By incorporating sodium iodide we found that fluorescence dropped well below that of controls and the results from our quenching suggest that this was largely a result of protein thiol oxidation as opposed to fluorescence interference (Figure 6). The mechanism of this catalytic reaction with sodium iodide still remains unclear however it appears that iodide may mediate electron transfer between thiols and H₂O₂⁹⁷.

Appendix B: Supplemental figures



Supplemental Figure 1. Representative image of redox western on mouse cardiac lysate in phosphate buffer (pH 7.5) with samples incubated with 5mM DTT and 5mMH₂O₂. 100nM IRDye per sample.

Appendix C: Buffers

Tris buffer

Chemical	Final Concentration (mM)
Tris	144.5
MgCl ₂	1.44

***pH to 7.1 at 4⁰C**

Chaps buffer

Chemical	Final Concentration
NaCl	120mM
NaF	50mM
HEPES	40mM
B-glycerophosphate	10mM
NaHP ₂ O ₇ •H ₂ O pyrophosphate	10mM
CHAPS	0.30%

***pH to 7.5**

Heat treatment buffer

Chemical	Final Concentration (mM)
NaCl	145
Hepes	10
KCl	3
CaCl ₂	2.5

***pH to 7.4**

Tris BSAN buffer (for HPLC measures)

Chemical	Final Concentration (mM)
Tris	50
Boric Acid	20
Acivicin	20
NEM	5
L-Serine	2

Appendix D: Homogenization protocol

1. Place muscle in metal dish filled with liquid nitrogen
2. Using pre chilled spatula chip piece of muscle of desired size
3. Using pre chilled forceps quickly place muscle on scale to get rough weight (do not wait for steady weight). While weighing, place forceps back in liquid nitrogen to remain cool
4. After getting weight, place muscle back in liquid nitrogen storage dewer until all samples have been weighed
5. Using the following dilution protocol place muscle in desired volume of homogenization buffer that contains:

1:100 Phosphatase Inhibitors 2 and 3

1:200 Protease Inhibitors

6. Dilutions: 300uL CHAPS buffer/30-40mg of muscle
7. Fill 50mL beaker with ice and place eppendorf with muscle securely in ice
8. Homogenize using tapered pestle for 2x30 seconds
9. Centrifuge at 13,500g for 10 minutes at 4°C

Appendix E: Final protocol for treatment with TCEP and H₂O₂

1. Weigh 40 mg of cardiac muscle
2. Put the tissue in 1.5 ml tube and 0.3 ml ice cold Tris buffer containing protease inhibitors
3. Mince tissue with fine scissors and homogenize on ice for 2 x 30s. Repeat for another 30s if necessary.
4. Spin down for 10 min at 13,500 rpm
5. Collect supernatants and run each sample through 2 successive desalting Zeba columns to remove endogenous glutathione (and other dye-interfering factors)
6. Determine protein concentration using BCA assay
7. Dilute samples to 4.167mg/ml in 200µl total volume
8. Add 1mM TCEP and 5mM H₂O₂+NaI to their respective samples
9. Incubate all samples together on a rocking platform for 5 minutes at room temperature
10. Run each sample again through 2 successive desalting Zeba columns to remove excess reagents
11. Determine protein concentration using reducing-agent compatible BCA assay
12. Dilute samples to 1mg/ml and label with 400nM IRDye800CW Maleimide
13. Incubate overnight
14. Next day remove excess dye by spinning through 2 successive desalting Zeba columns
15. Determine protein concentration and proceed with western blotting protocol

Appendix F: BCA protein assay

1. Create protein standards by diluting BSA in homogenization buffer
2. Standards (BSA):

0 mg/mL (buffer)

0.0625 mg/mL

0.125 mg/mL

0.25 mg/mL

0.50 mg/mL

0.75mg/mL

1.00 mg/mL

3. Dilute 5 μ l of each sample in 45 μ l of homogenization buffer
4. Using a 96-well plate load 10 μ l in triplicates each standard and each sample
5. Add 190 μ l of working reagent (50:1 Solution A:SolutionB) into each well of sample
6. Heat in over for 30 minutes at 37°C

Reducing agent compatible (RAC) BCA assay

1. Prepare a sample (without protein) containing reducing agent at the same concentration as experimental samples
2. Repeat steps 1-3 above for all samples
3. Using a 96-well plate load 9 μ l of each standard and sample in triplicates
4. Add 4 μ l of Compatibility Reagent (reconstitution buffer + compatibility reagent) to each sample in each well
5. Incubate plate for 15 minutes at 37°C
6. Add 260 μ l of working reagent to each well and incubate for 30 minutes at 37°C

Appendix G: Western blotting protocol

Gel preparation

1. In 50mL falcon tubes make running gel and stacking gel (1 column makes 2 gels) ***DO NOT ADD TEMED UNTIL READY TO LOAD**
2. Take 1 short plate and one spacer plate and clean both sides of glass with methanol and kimwipe
3. Place clean short plate on top of spacer place and place both in mounting apparatus, ensuring the edge of the plates are lined up against the bench top
4. Place plates in apparatus on foam piece in gel stand
5. Place 3 transfer pipettes and falcon tube with methanol close to gel stand

	<i>Stacking</i>	<i>Running</i>				
		5%	6%	8%	10%	12%
<u><i>dH₂O</i></u>	6.8 ml	11.4	10.6 ml	9.4 ml	8 ml	6.7 ml
<u><i>1.5M Tris-Base, pH 8.8</i></u>	***	5 ml	5 ml	5 ml	5 ml	5 ml
<u><i>1M Tris-HCl, pH 6.8</i></u>	1.25 ml	***	***	***	***	***
<u><i>30 % Acrylamide</i></u>	1.70 ml	3.4 ml	4 ml	5.3 ml	6.7 ml	8 ml
<u><i>10 % SDS</i></u>	100 µl	200 µl	200 µl	200 µl	200 µl	200 µl
<u><i>10 % APS</i></u>	100 µl	200 µl	200 µl	200 µl	200 µl	200 µl
<u><i>Temed</i></u>	20 µl	20 µl	20 µl	20 µl	20 µl	20 µl

6. Add TEMED to running gel and invert falcon tube 1-2 times

7. Using transfer pipette, fill space between glass plates with running gel until solution reaches the top of the green doors
8. Using new transfer pipette add methanol to top of plate to create an even line along the top of the gel removing any bubbles
9. Let sit until remaining running gel has set in the flask tube
10. Once gel has hardened, invert gel to remove any excess methanol
11. Add TEMED to stacking gel and mix
12. Using transfer pipette, add stacking gel to top of glass plates, use methanol transfer pipette to remove any bubbles
13. Add comb to top of gel and allow to set
14. Prepare diluted samples by combining sample, water and Laemmli's buffer + 2-mercaptoethanol (100 μ l 2-mer: 900 μ l Lam)
15. Spin down samples for 5 seconds
16. Make 1X running buffer in 1000mL graduated cylinder
17. Remove combs from gels and place gels in gasket
18. Place gasket with gels in tank and add 1X running buffer until it fills the top of gasket and tank
19. Load wells with desired concentration of samples
20. Run for desired time (40-75 minutes) at 160mV (or desired voltage) and protect from light
21. When run is complete, carefully remove gel, rinse with TBST to remove small bubbles from surface
22. Detect using LiCOR Infrared Imager